Inelastic electron tunneling study of UV radiation damage in surface adsorbed nucleotides

James M. Clark and R. V. Coleman

Citation: The Journal of Chemical Physics **73**, 2156 (1980); doi: 10.1063/1.440411
View online: http://dx.doi.org/10.1063/1.440411
View Table of Contents: http://scitation.aip.org/content/aip/journal/jcp/73/5?ver=pdfcov
Published by the AIP Publishing

Articles you may be interested in

Identifying configuration and orientation of adsorbed molecules by inelastic electron tunneling spectra
J. Chem. Phys. **133**, 064702 (2010); 10.1063/1.3474807

Simulation of inelastic electronic tunneling spectra of adsorbates from first principles
J. Chem. Phys. **130**, 134707 (2009); 10.1063/1.3106235

Inelastic electron tunneling spectroscopy of silane coupling agents adsorbed on alumina
J. Chem. Phys. **83**, 5981 (1985); 10.1063/1.449631

The reaction of ethanol with an aluminum oxide surface studied by inelastic electron tunneling spectroscopy
J. Chem. Phys. **71**, 1537 (1979); 10.1063/1.438496

Electron Microscope Study of Radiation Damage in Graphite
J. Appl. Phys. **32**, 869 (1961); 10.1063/1.1736121

This article is copyrighted as indicated in the article. Reuse of AIP content is subject to the terms at: http://scitation.aip.org/termsconditions. Downloaded to IP: 128.83.63.20 On: Thu, 27 Nov 2014 09:56:33

Inelastic electron tunneling study of UV radiation damage in surface adsorbed nucleotides

James M. Clark and R. V. Coleman

Physics Department, University of Virginia, Charlottesville, Virginia 22901
(Received 19 November 1979; accepted 16 May 1980)

Ultraviolet radiation damage to nucleotides has been studied using inelastic electron tunneling (IETS) to monitor the direct bond damage as reflected in the vibrational mode intensity. The damage rate is found to be directly correlated to the resonance energy per π electron of the purine or pyrimidine base residue. Low lying ring modes are damaged most rapidly while modes associated with CH components are less rapidly damaged. The mononucleotides are damaged more rapidly than the corresponding bases, but no cleaving of the glycodidic bond between the base and sugar is observed. In the case of the purine base nucleotides double bond structure develops during UV exposure and is attributed to the more complex damage sequence of the base ring. The nucleotides are adsorbed on the alumina barrier of an Al–AlO_x–Pb tunnel junction and the PO_2^- group interacts with the surface. The majority of the other vibrational modes are unperturbed and indicate that the sugar and base rings form a complex on the surface of relatively fixed orientation. The IETS spectra of all nucleotides indicate a similar surface adsorption and this is not influenced by variation of the substrate temperature as is the case for molecules with a less constrained surface orientation. This unique surface configuration is discussed along with comparison to other molecules where temperature effects on the IETS spectrum are strong. Preliminary results of UV damage to polynucleotides and polypeptides is also reported. The role of the alumina surface structure and interaction with respect to the different types of molecules is also discussed.

I. INTRODUCTION

The effects of ionizing and nonionizing radiation on biological systems have been studied using a variety of techniques.[1,2] Traditionally, chemical and chromatographic methods have been employed to detect and identify radiation products of the radical, monomeric, and dimeric forms. On the atomic scale the chief tool has been electron spin resonance. More recently, infrared spectroscopy of bulk films of nucleic acids and their components has provided information about selective bond damage and commensurate changes in molecular structure. In this paper, we present results obtained by inelastic tunneling spectroscopy (IETS) which further reinforce the potential role of vibrational spectroscopy in the study of radiated biological systems.

The use of IETS to study radiation effects on organics has been previously demonstrated. Hansma and Parikh[3] used the technique to identify changes in the molecular structure of β-*D*-fructose after exposure to an electron beam and Simonsen[4] studied proton damage to TCNQ. Hall *et al.*[5] radiated simple carboxylic acids with electrons and showed clearly the correlation of structural damage with the degree of π electron delocalization in the acids. In contrast to bulk results, the tunneling results showed little if any evidence of crosslinking following irradiation. Evidence for conjugation was present in the case of β-*D*-fructose.[3]

IETS involves the fabrication and measurement of a metal–insulator–metal tunnel junction (usually Al–AlO_x–Pb). Prior to deposition of the top metal, the molecules under study are placed on the surface of the insulator as an adsorbed layer equivalent to approximately a monolayer. In response to an applied voltage, electrons tunnel through the insulator and molecular layer and provide information about the inelastic interactions with the molecules. Although the resolution of IETS is no greater than that of the conventional optical spectroscopies, the small sample thickness required in IETS results in much higher sensitivity. The thin sample layer should also be advantageous in a radiation experiment since the adsorbed molecules are more uniformly exposed to the incoming flux.

The fact that the molecules are adsorbed on an alumina substrate and overlaid with a lead electrode would be expected to produce deviations in the tunneling spectra from that observed for the free molecule. The primary effect of the lead electrode is to downshift the tunneling modes due to an image dipole induced in the electrode.[6] For the internal vibrations of a complex molecule, these shifts are smaller than the resolution. Reaction of the molecules with the alumina substrate is reflected in the formation of new bonds and therefore new vibrational modes. For example, benzaldehyde and benzoic acid adsorb on alumina to form a benzoate ion.[7] Both the Raman-type and infrared-type interaction can contribute comparable intensity in IETS and agreement with infrared and Raman results is generally good.[7,8]

We have previously reported results of ultraviolet radiation damage to uridine 5′-monophosphate using IETS.[9] In this paper we present a more in-depth study of the primary radiation effects of ultraviolet light on nucleic acid constituents and peptides. We have also carried out a more complete evaluation of the technique for use in an application of this type and will point out a number of the unique aspects. Molecules adsorbed on the surface of the alumina substrate have been radiated directly under ultrahigh vacuum conditions. Molecular damage is measured by a loss of intensity in the vibrational structure due to bond weakening or breaking and an enhancement in the intensity of modes associated with

 0021-9606/80/172156-23$01.00 © 1980 American Institute of Physics

This article is copyrighted as indicated in the article. Reuse of AIP content is subject to the terms at: http://scitation.aip.org/termsconditions. Downloaded to IP: 128.83.63.20 On: Thu, 27 Nov 2014 09:56:33

new radiation products. An assessment of the role of the alumina surface is also presented.

II. EXPERIMENTAL TECHNIQUES

Al–AlO_x–Pb tunnel junctions were fabricated according to the following procedure. Five aluminum strips ~2000 Å thick and 0.22 mm wide were evaporated onto a clean microscope slide in an oil diffusion-pumped high vacuum system at 10^{-6} Torr. The strips were thermally oxidized in air under a laminar flow hood to form the tunnel barrier. A drop of dilute solution containing the dopant molecule was placed on each oxidized strip and the excess spun off following the liquid doping method developed by Hansma and Coleman.[10] The center junction was not doped and served to monitor contamination. After doping, the slide was returned to vacuum and the junctions completed by evaporating a lead strip (~1 μm thick) crosswise over the barrier and molecules. Typical resistances for doped junctions ranged from 50–2000 Ω; resistances for undoped junctions were 1–2 Ω. Dopant chemicals were obtained from Calbiochem and PL Biochemicals and were used without further purification.

For junctions which were irradiated, the initial fabrication steps were carried out as described above. After doping the slide was mounted on a copper sample block in an ion-pumped ultrahigh vacuum system equipped with a titanium sublimator for rapid pumpdown. System pressures in the 10^{-8} Torr range could be attained within 7–10 min. The copper block was fixed directly to a vacuum Dewar and was cooled with liquid nitrogen before each irradiation to reduce sample heating. A junction on one end of the slide was radiated with UV; the junctions on the opposite end were not exposed and served as control junctions. Immediately following the irradiation the lead electrode was evaporated in place. The geometry of the experimental apparatus (primarily the spread of the light beam) allowed only one junction to be radiated during a particular run.

The interaction of the tunneling electrons with the organic molecules exhibits peaks in the second derivative characteristic d^2V/dI^2 vs V of the junction at energies corresponding to the vibrational frequencies of the adsorbed molecules. Completed junctions were measured at 4.2 K. The second derivative is measured by applying a small ac signal (0.5–2 mV) to the junction and detecting the second harmonic voltage with a lock-in amplifier. The second harmonic is proportional to d^2V/dI^2 which in turn is related to the infrared and Raman spectral weight densities. The IETS spectra were recorded by sweeping the range 200–3800 cm^{-1} in a period of 70 min with a lock-in sensitivity of 1 μV (full scale) and a 3 sec time constant. The vibrational frequencies, accurate to within ±5 cm^{-1}, were recorded and corrected by −8 cm^{-1} to account for the shift due to the superconducting gap of the lead electrode. A complete discussion of the fabrication and measurement techniques used in IETS may be found in Refs. 7 and 8.

The UV source was a 1000 W xenon–mercury compact arc lamp (Hanovia 977B). The slightly defocused output of the lamp was directed full strength (a monochromator was not used) onto the barrier and adsorbed molecules through an infrared filter (triply distilled water, 4 in. optical path length). The spread of the beam with respect to the width of the aluminum strips insured uniform exposure over the barrier. Using lamp curves and transmittance values the radiation fluences were calculated to be 10 J/cm^2 for a 1 min exposure and 600 J/cm^2 for a sixty minute exposure. If the average photon wavelength is assumed to be ~2500 Å then a one minute exposure would correspond to a fluence of $\sim 1.26\times10^3$ photons/$Å^2$. Typical irradiation exposure times ranged from 0 to 60 min at pressures of 7×10^{-9} to 2×10^{-8} Torr.

III. IETS SPECTRA OF PYRIMIDINES, PURINES, AND NUCLEOTIDES

The infrared and Raman spectra of nucleic acid constituents have been reported in great detail[11,12]; the IETS spectra of nucleosides and nucleotides have also been reported.[13] The complexity and low symmetry of the molecules make band assignments difficult. Group frequency identifications have traditionally been made by studying a series of closely related derivatives and using isotopic substitutions, methylation, and pH variations to deduce the origin of the modes. We have used the results of these former experiments to assign the major vibrational structure in the IETS spectra of the purine and pyrimidine bases and hence to demonstrate the correspondence between IETS and the optical spectroscopies.

A. Pyrimidines

The tunneling spectra of uracil, thymine, and cytosine and their 5′-nucleotides are shown in Figs. 1, 2, and 3 respectively. The wave numbers for the bases and nucleotides are identified in Tables I, II, and III along with a comparison to Raman and infrared data. All of the tunneling spectra were obtained by doping a junction from an aqueous solution of the base or nucleotide. In general, the bases do not adsorb strongly and their poor solubility properties in water make it difficult in some cases to obtain a high resistance tunnel junction. The cytosine junction was 932 Ω, while the uracil and thymine junctions were 56 and 50 Ω, respectively. In spite of the somewhat low resistances in the latter cases, the tunneling spectra are very good and allow a reliable mode identification.

The detailed adsorption of the bases and nucleotides on alumina is uncertain. The most probable mechanism for bonding is coordination at the aluminum ion site on the surface by the ring nitrogen or oxygen substituent. Studies of the bonding of heavy metal ions to pyrimidine bases in solution indicates that coordinate bonding occurs at the ring nitrogen (the most basic site). Steric considerations imposed by the surface also make the oxygen substituent a candidate. The strongest modes in the tunneling spectra are generally attributed to the ring and to C–H structure. The very strong peak at 432 cm^{-1} is characteristic of all the pyrimidine bases on alumina and is assigned to a ring deformation mode.

The Raman frequencies attributable to the base rings have been identified by Lord and Thomas.[11] For uracil, strong polarized lines are observed near 790 and 1235

This article is copyrighted as indicated in the article. Reuse of AIP content is subject to the terms at: http://scitation.aip.org/termsconditions. Downloaded to IP: 128.83.63.20 On: Thu, 27 Nov 2014 09:56:33

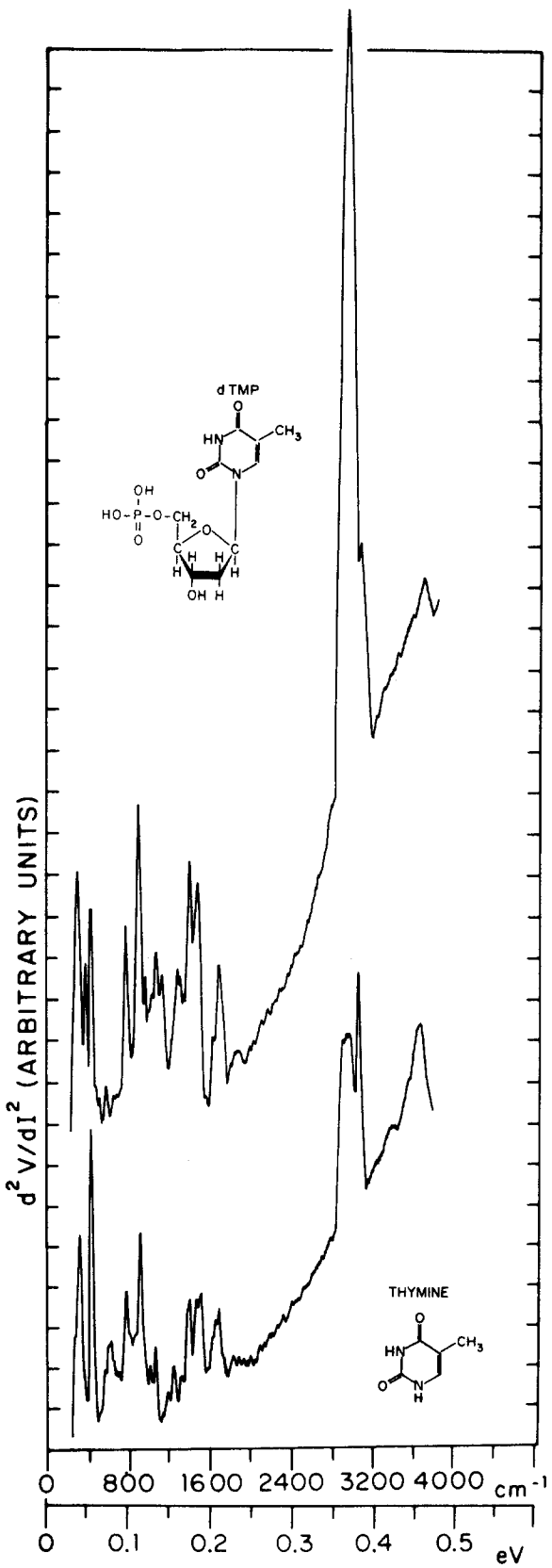

FIG. 1. IETS spectra of 5′-dTMP (upper spectrum, 539 Ω) and thymine (lower spectrum, 50 Ω). Both spectra were recorded using Al–AlO_x–Pb junctions doped from H_2O solutions. Spectra were recorded with the junction at 4.2 K.

cm^{-1}; the tunneling spectrum of uracil exhibits medium intensity peaks at 794 and 1234 cm^{-1}. In the IETS spectrum of cytosine peaks assigned to the ring are at 799 (strong) and 1290 cm^{-1} (medium). Out-of-plane C–H deformation modes should appear in the 750–825 cm^{-1} range and are weak in Raman spectra and strong in the infrared. Uracil and cytosine both show strong modes near 730 cm^{-1} in the IETS spectra and these are assigned to C–H deformation modes although they are somewhat low. A mode at 819 cm^{-1} in the uracil tunneling spectrum is also assigned to a C–H deformation mode. Peaks at 790 and 730 cm^{-1} are not present in the tunneling spectrum of thymine; instead a strong mode appears at 766 cm^{-1}. The character of this mode is probably C–H deformation but a contribution from the ring is also likely.

Ring stretching motions and ring C–H and N–H in plane bending motions in the range 1300–1500 cm^{-1} are

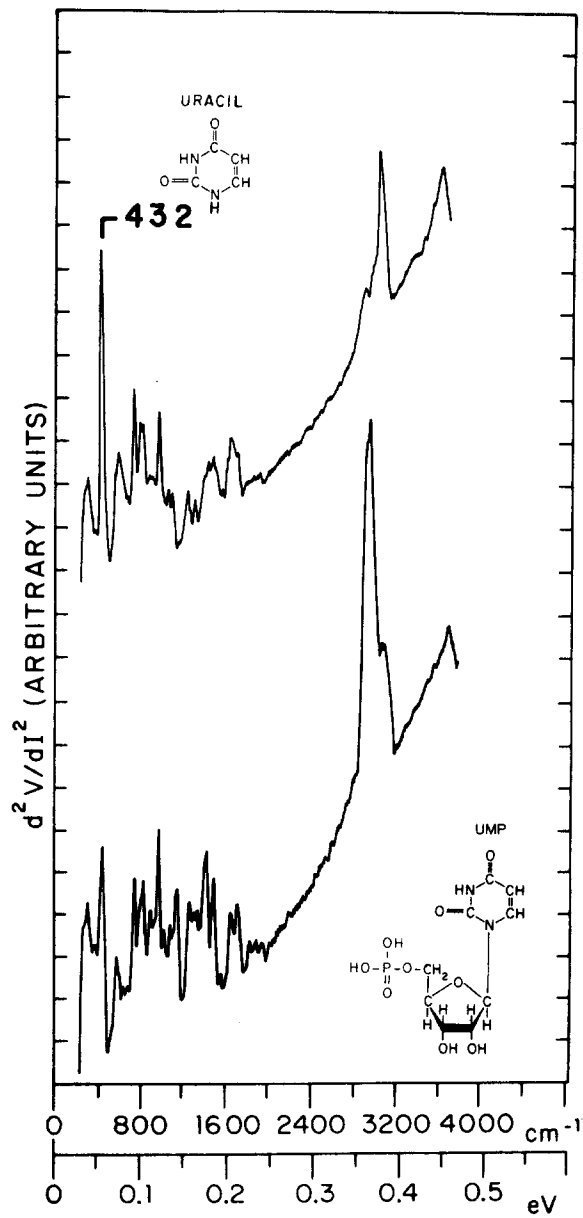

FIG. 2. IETS spectra of 5′-UMP (lower spectrum, 695 Ω) and uracil (upper curve, 56 Ω). Both spectra were recorded at 4.2 K from Al–AlO_x–Pb junctions doped from H_2O solutions.

This article is copyrighted as indicated in the article. Reuse of AIP content is subject to the terms at: http://scitation.aip.org/termsconditions. Downloaded to IP: 128.83.63.20 On: Thu, 27 Nov 2014 09:56:33

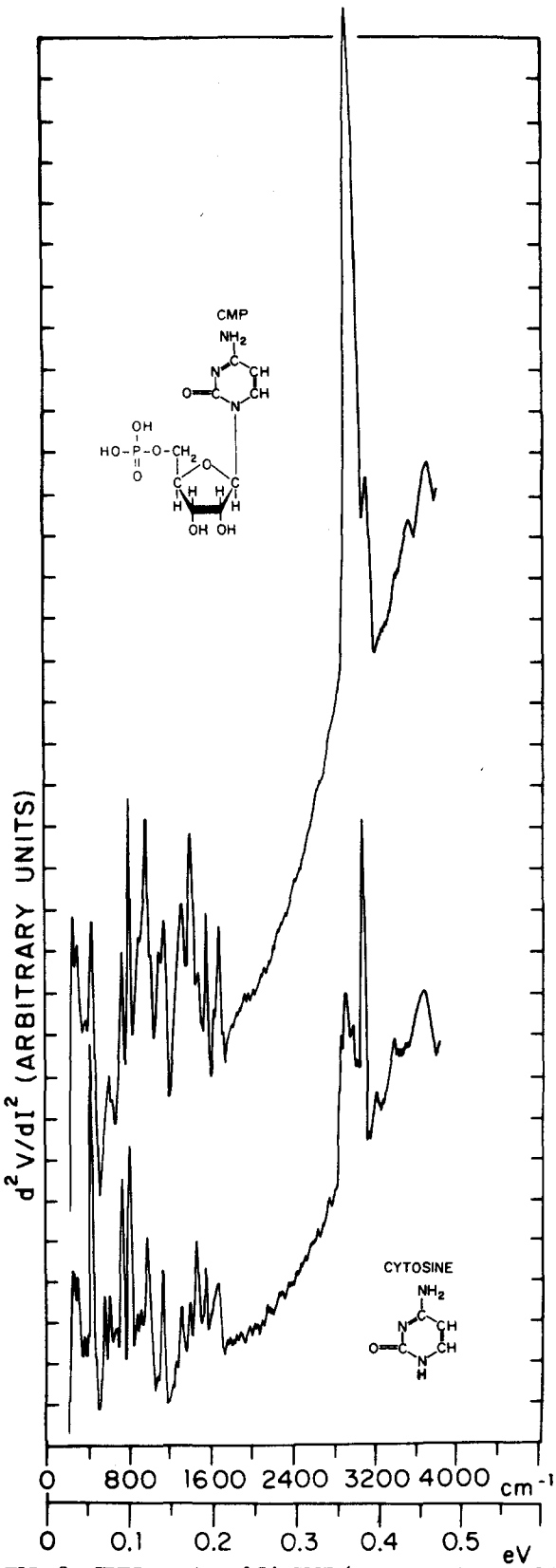

FIG. 3. IETS spectra of 5′-CMP (upper spectrum, 1274 Ω) and cytosine (lower spectrum, 932 Ω). Both spectra were recorded at 4.2 K from Al–AlO_x–Pb junctions doped from H_2O solutions.

identified in the infrared and Raman spectra. The tunneling spectrum of uracil exhibits peaks at 1399 and 1440 cm^{-1} which are not well resolved while the tunneling spectrum of cytosine exhibits a peak at 1371 cm^{-1} and a much stronger peak at 1440 cm^{-1}. In both cases the lower of these modes is assigned to the ring and the 1440 cm^{-1} mode is assigned to a ring C–H bending mode. However, Susi *et al.*[14] have shown by preferentially deuterating the N–H and C–H groups that the reverse assignments may be more accurate. Thymine shows peaks at 1359, 1379, and 1452 cm^{-1}. It is likely that the symmetric and asymmetric bending vibrations of the substituent methyl group ($-CH_3$) contribute strongly at 1379 and 1452 cm^{-1}, while the mode at 1359 cm^{-1} can be identified with the ring C–H bending mode. Bending vibrations of the N–H groups coupled with the ring vibrations are observed at 1492 cm^{-1} in thymine and at 1500 cm^{-1} in uracil.

The strong tunneling mode at 1528 cm^{-1} in cytosine is not present in uracil or thymine. Angell[15] has identified the mode as an NH deformation and attributed the motion principally to N_1–H since the mode became weak on substitution at N_1. Lord and Thomas[11] have identified the mode as a skeletal ring vibration involving mainly C=N

TABLE I. IETS, Raman, and IR wave numbers (cm^{-1}) for uracil and 5′-UMP.

Uracil			5′-UMP (sodium)		
Raman[a] (solid)	IETS	ir[a]	Raman[b] (H_2O, *p*H 7.4)	IETS	ir[c]
	266 m[d]			254	
	303 m			290	
398(0.2)[d]	371 w			367	
431(1.0)	432 vs	435 s		428	
				528	
531(1.0)		530 w	558	565	
540(1.3)		550 s		589	
558(2.6)	565 sh	565 m	640	621	673
579(2.5)	589 m	585 m		726	732
	653 w		784	786	760
	682 w		810	811	810
771(0.1)	734 s	760 s			833
792(10)	794 ms	781 w	880	875	869
		807 m			891
830(0.3)	819 ms	822 s	982	952	973
867(0.1)	895 w	851 m	1000	1004	997
988(0.8)	964 s	993 m			1020
1010(0.4)	1053 w	1003 m			1042
1104(0.1)	1089 w	1099 w		1065	1075
		1217 w			1101
1236(10)	1234 m	1238 s	1125	1117	1124
	1299 w				1203
1398(3.4)	1399 w	1390 m	1232	1242	1247
1422(1.5)		1417 s			1260
1462(1.0)	1440 wm	1453 s		1286	1282
	1480 wm			1311	1314
1507(0.8)	1500 sh	1508 m	1397	1391	1379
	1569 w				1412
1611(0.4)	1605 sh		1470	1460	1466
1648(2.0)	1645 m			1532	
1662(1.4)		1675 s		1585	
	1702 m	1716 s	1640	1653	
3085(1.0)	2895 m	3080 s	1680	1686	1686
3100(1.0)	3045 s	3100 s			1724
3130(0.1)		3160 m			

[a]H. Susi and J. S. Ard, Spectrochim. Acta Part A **27**, 1549 (1971).

[b]R. C. Lord and G. J. Thomas, Jr., Spectrochim. Acta Part A **23**, 2551 (1967).

[c]C. L. Angell, J. Chem. Soc. 504 (1961).

[d]Key: br, broad; sh, shoulder; w, weak; m, medium; s, strong; vs, very strong. Numbers in parentheses indicate strengths of Raman lines on scale of 0 to 10 (strongest).

This article is copyrighted as indicated in the article. Reuse of AIP content is subject to the terms at: http://scitation.aip.org/termsconditions. Downloaded to IP: 128.83.63.20 On: Thu, 27 Nov 2014 09:56:33

TABLE II. IETS, Raman, and IR wave numbers (cm^{-1}) for thymine and 5′-dTMP.

Raman[a] (solid)	Thymine IETS	ir[b]	5′-dTMP (sodium) IETS
	266 sh[c]		294
321	319 s		375
475	432 vs		423
562	561 w		504
	589 w		565
618	613 w		
	645 sh		641
	694	740 m	678
866	766 ms	762 s	710
		815 s	766
	907 s	845 s	891
	948 sh	935 m	956
985	996 w	983 m	
		1029 m	1012
	1049 m	1048 w	1057
1157	1161 w		1117
1216	1222 m	1205 s	1178
1248	1299 w	1244 s	1230
1370	1359 sh	1366 w	1258
1379	1379 ms	1381 m	1286
1409		1422 s	1323
1461	1452 m	1447 s	1383
		1484 m	1468
1492	1492 ms	1495 m	1545
1600	1605 wm		1617
	1633 m		
1674	1670	1681 s	1670
1706		1739 s	1710
		1785 w	
	2887 s	2800 w	
2934	2912 s	2920 m	
2991	2948 s	3020 s	2936
3066	3041 s	3170 m	3041
			3085

[a]H. Susi and J. S. Ard, Spectrochim. Acta Part A **30**, 1843 (1974). These lines were identified by Susi and Ard to be in-plane modes.
[b]C. L. Angell, J. Chem. Soc. 504 (1961).
[c]Key as in Table I.

stretching. X-ray studies however indicate that the C=N bond is only slightly shorter than neighboring single bonds and would be expected to couple with ring stretching modes rather than exhibit a separate double bond vibration. In the tunneling spectrum the mode is equally strong in both 5′-CMP (Fig. 3, upper curve) and cytosine and probably possesses both ring and NH character. Another tunneling mode at 1113 cm^{-1} is also unique to cytosine, and contributions at this frequency come from the ring and the NH_2 rocking vibration.

The double bond stretching region (1500–1750 cm^{-1}) contains vibrations from C=C, C=N, and the conjugated and nonconjugated carbonyl groups. The scissoring vibration of the amino group of cytosine is also present in this region. In the tunneling spectrum of uracil a mode at 1702 cm^{-1} is assigned to $\nu(C_2{=}O)$ and at 1645 cm^{-1} to $\nu(C_4{=}O)$. Thymine exhibits these peaks at 1670 and 1633 cm^{-1}. A similar assignment is possible in this case but is more uncertain since these modes are downshifted from the corresponding ir and Raman modes (see Table II). A peak at 1605 cm^{-1} in both bases can be assigned to the C=C stretch mode. In cytosine, the C=O group is conjugated and a peak at 1645 cm^{-1} is attributed to ν(C=O) since the mode occurs at the same frequency as the conjugated carbonyl stretch in uracil. The NH_2 scissoring vibration in cytosine is not separately resolved, but the presence of the amino group is confirmed by the NH_2 stretch modes at 3186 (symmetric) and 3351 cm^{-1} (asymmetric).

The strong peak at 964 cm^{-1} in the IETS spectra of uracil and cytosine and at 907 cm^{-1} in thymine arises from the alumina phonon modes. In an undoped junction this mode is strong and very broad reflecting the presence of similar but inequivalent structure in the barrier. In doped junctions this mode may vary both in frequency and intensity depending on the nature of the dopant molecule. These variations indicate that the alumina phonon modes are influenced by the detailed bonding of the adsorbate to the active sites on the alumina surface. Consequently, this mode reflects the net barrier structure

TABLE III. IETS, Raman, and IR wave numbers (cm^{-1}) for cytosine and 5′-CMP.

			5′-CMP		
Raman[a] (H_2O, pH 7)	cytosine IETS	ir[b]	Raman[a] (H_2O, pH 9)	IETS	ir[c]
	250[d]			235	
	298 m			290	
	367 w	421 w	400	371	
	432 vs	442 w	553	432	
		520 sh	600	605	
		533 m	635	633	681
546(2)[d]	557 m	549 m	710	726	717
		566 w			755
590(1)	605 m	600 m			773
	669 w	701 w	783	794	786
	726 s	760 sh	810		808
		782 m			837
787(10)	799 s	793 m	875	883	870
	867 w	823 m			905
	907 w			924	931
975 (1)	964 s	966 w	983	956	
		994 w	995	996	988
	1065 w	1010 w			1016
1125(2)	1113 s	1100 w			1048
	1206 w				1069
1228(2)	1238 w	1236 m	1055	1085	1093
1290 (10)	1290 m	1277 m	1130	1125	1111
1365(2)	1371 wm	1364 m	1190		1161
1440(1)	1440 ms	1465 s	1215		1222
		1505 m	1243	1234	
1530(2)	1528 m	1538 m		1266	1255
	1593 sh	1615 s	1294	1294	1279
1660 (2br)	1645 m, br	1662 vs			1333
		1703 w	1375	1375	1351
	2851 m		1415		
	2891 m		1460	1452	
	2960 m			1492	
	3057 vs		1530	1536	1545
	3186 w	3169 s	1585		
	3351 w, br	3380 s	1605	1613	1605
					1626
			1655	1653	
					1704
					1724

[a]R. C. Lord and G. J. Thomas, Jr., Spectrochim. Acta Part A **23**, 2251 (1967).
[b]H. Susi, J. S. Ard, and J. M. Purcell, Spectrochim. Acta Part A **29**, 725 (1973).
[c]C. L. Angell, J. Chem. Soc. 504 (1961).
[d]Key as in Table I.

This article is copyrighted as indicated in the article. Reuse of AIP content is subject to the terms at: http://scitation.aip.org/termsconditions. Downloaded to IP: 128.83.63.20 On: Thu, 27 Nov 2014 09:56:33

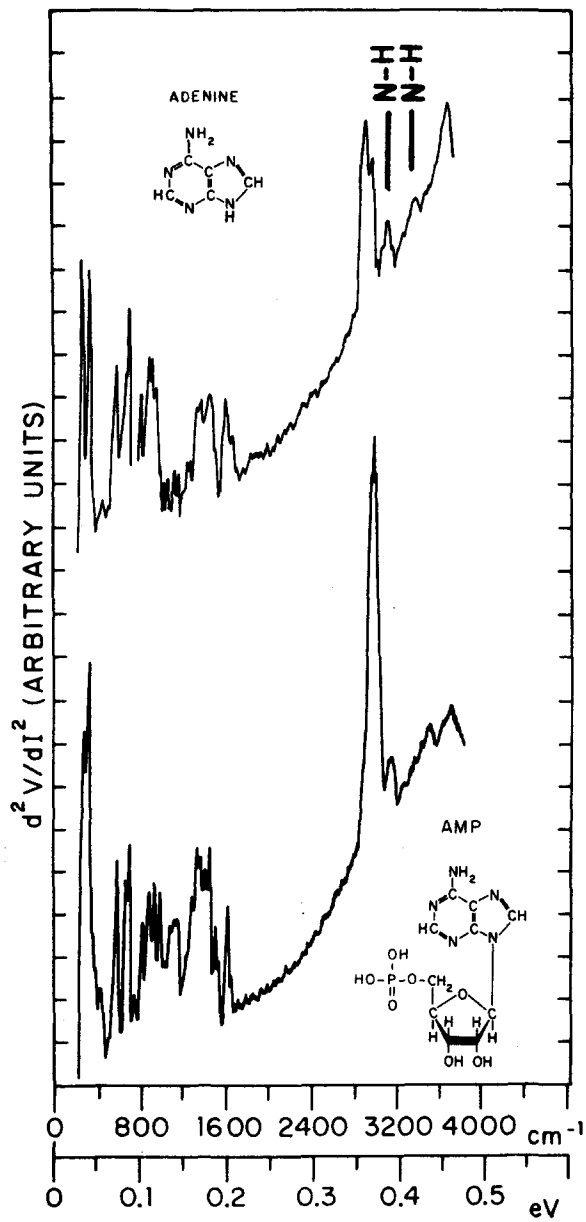

FIG. 4. IETS spectra of 5′-AMP (lower spectrum, 1818 Ω) and adenine (upper curve, 498 Ω). Both spectra were recorded at 4.2 K from Al–AlO_x–Pb junctions doped from H_2O solutions.

including modifications resulting from the molecular adsorption process. In the sections that follow, the reader should pay particular attention to the influence of UV on this mode.

B. Purines

The IETS spectra of adenine and 5′-AMP are shown in Fig. 4, and the wave numbers of adenine are listed in Table IV along with the results of infrared and Raman measurements. In the tunneling spectrum of adenine coupled C=C and C=N motions are observed at 1540, 1577, and 1601 cm^{-1}. A peak at 1645 cm^{-1} is assigned to the NH_2 scissoring vibration and is resolved in adenine in contrast to cytosine. Modes in the 1300–1500 cm^{-1} range are ring and C–H bending modes and appear as a series of five peaks superposed on a broad envelope. In the spectrum of 5′-AMP, the peaks are well resolved. Medium intensity peaks at 799 and 871 cm^{-1} in adenine are attributed to C–H deformation motions.

The tunneling spectrum of adenine shows a strong mode at 690 cm^{-1} and shoulders at 625 and 649 cm^{-1}. The mode at 690 cm^{-1} has been assigned by others to the NH_2 wagging vibration. In the tunneling spectrum of inosine (which has an OH group in place of the NH_2 group) these modes are replaced by two strong peaks at 649 and 700 cm^{-1}. Though the NH_2 wagging vibration may be coupled to the mode at 690 cm^{-1} in adenine, the dominant character of this mode in the tunneling spectrum does not come from the amino group. It is reasonable, based on Raman results and anisotropy studies of single crystals, to associate the strong peaks below 700 cm^{-1} in the spectrum of adenine with internal vibrations of the ring.

A satisfactory spectrum of guanine was not obtained despite attempts to enhance its solubility properties by *p*H adjustments. The spectrum of 5′-GMP was recorded and is shown in Fig. 5. The spectrum is more diffuse than that of AMP, but still a number of modes can be

TABLE IV. IETS, Raman, and IR wave numbers (cm^{-1}) for adenine and 5′-AMP.

	Adenine		5′-AMP		
Raman[a] (solid)	IETS	ir[b]	Raman[a] (H_2O, *p*H 7)	IETS	ir[b]
	242 vs[c]			242	
334(2)[c]	319 vs			287	
	444 w		320	352	
535(2)	536 sh			408	
	569 s			500	
620(2)	625 sh		538	528	
	649 m		575	570	
	690 s		635	653	
725(5)	734 w	722 m		682	683
820(0)	799 m	797 m	710		725
		847 m	730	734	737
	871 m	870 w			787
900(0)	899 m	911 m	800	803	822
945(2)	940 m	938 m	820		831
	984 sh		890	855	893
1025 (1br)	1024 w	1022 m	915	911	913
	1065 w				930
1130(2)	1117 w	1124 m	980	960	966
	1153 w	1155 w	1000		1020
		1206 m	1050	1065	1064
1225(1)	1238 m		1090	1097	1089
1252(5)		1250 m		1121	1114
1312(2)		1305 m	1180	1186	1170
1332(10)	1355 wm	1333 m	1220	1214	1219
1370(2)	1363 wm	1368 w	1253	1258	1250
	1411 wm	1418 m			1294
1462(2)	1448 m	1451 w	1308	1311	1317
1485(5)	1480 sh		1340	1339	1345
1530(0)	1540 w	1510 w	1380	1379	1402
	1577 sh		1425	1420	1422
1600(2)	1601 m	1605 m	1485	1484	
	1645 m, sh	1672 s	1510	1508	1500
	2879 s	2680 w			1562
	2928 m	2780	1583	1593	1613
	2956 m	3000 w	1640	1641	1700
	3093 br	3105 s			
	3335 br	3280 m			

[a]R. C. Lord and G. J. Thomas, Jr., Spectrochim. Acta Part A **23**, 2251 (1967).
[b]C. L. Angell, J. Chem. Soc. 504 (1961).
[c]Key as in Table I.

This article is copyrighted as indicated in the article. Reuse of AIP content is subject to the terms at: http://scitation.aip.org/termsconditions. Downloaded to IP: 128.83.63.20 On: Thu, 27 Nov 2014 09:56:33

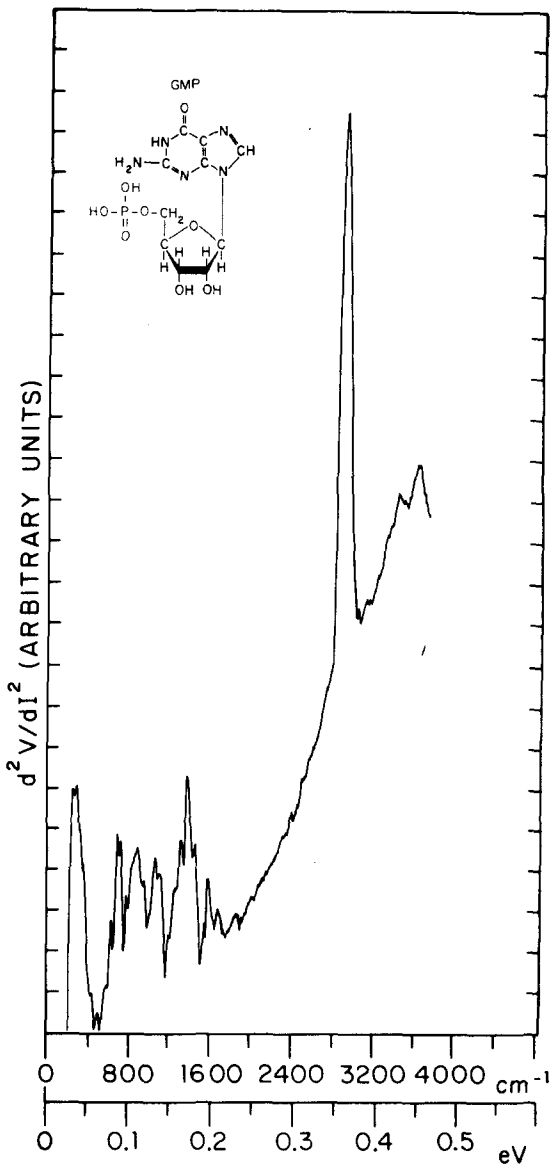

FIG. 5. IETS spectrum of 5′-GMP, 1302 Ω. Spectrum was recorded at 4.2 K from an Al–AlO_x–Pb junction doped from an H_2O solution.

identified, many of which exist as shoulder peaks. The C=O stretch mode can be seen at 1690 cm^{-1} and the NH_2 symmetric and asymmetric stretch modes at 3133 and 3460 cm^{-1}, respectively. Peaks at 1540, 1585, and 1601 cm^{-1} are coupled stretching vibrations of C=C and C=N. The strong peak at 698 cm^{-1} can tentatively be assigned to a symmetric skeletal vibration, but the intensity of this mode is at variance with the optical results. The IETS modes for 5′-GMP along with a comparison to ir and Raman results are listed in Table V.

C. Nucleotides

The solubility and adsorption properties of the bases are improved significantly by the attachment of sugar–phosphate moieties to form the nucleotides. Junction resistances of 1000 Ω are easily obtained, and the resistances reproduce consistently for a given dopant concentration. These features were of primary consideration in selecting the nucleotides rather than the bases as candidates for the radiation study using IETS.

The general features of the nucleotide IETS spectra, when compared to the base spectra, indicate that the dominant structure comes from the base rings. Alterations introduced by addition of the sugar–phosphate groups, aside from the specific mode contributions of these groups are limited to small shifts in the vibrational frequencies and variations in relative peak intensities. The shifts (~10 cm^{-1}) are of the same order as those observed in the infrared and Raman spectra of mononucleotides (see Ref. 12, Table I). IETS spectra of 5′-AMP, 5′-dTMP, 5′-CMP, 5′-UMP, and 5′-GMP were included in Figs. 1–5 and wave numbers for the IETS, Raman, and infrared modes observed for the nucleotides were listed in Tables I–V.

The specific mode contributions of the sugar groups to the nucleotide spectra appear in well defined regions of the spectra. Coupled C–O and C–C stretch modes are observed in the 1000–1125 cm^{-1} range. C–H and

TABLE V. IETS, Raman, and IR wave numbers (cm^{-1}) for 5′-GMP (disodium).

Raman[a] (H_2O, pH 7.5)	IETS	ir[b]
	266	
	294	
	367	
400	436	
502	512	
585	585	
	645	
675	698	692
	726	
	794	780
810	839	839
870	875	848
	891	917
	928	930
980		976
	1020	1030
		1057
1080	1069	1078
	1125	1127
1178	1194	1176
	1218	1235
1240	1254	
	1282	
1325	1323	1355
1367	1387	1380
1417		1416
1455	1456	
1490	1492	1481
1541	1540	1538
1578		
1605	1593	1608
1680	1690	1698
	2916	
	3133	3150
	3460	3425

[a]R. C. Lord and G. J. Thomas, Jr., Spectrochim. Acta Part A **23**, 2551 (1967).
[b]C. L. Angell, J. Chem. Soc. 504 (1961).

This article is copyrighted as indicated in the article. Reuse of AIP content is subject to the terms at: http://scitation.aip.org/termsconditions. Downloaded to IP: 128.83.63.20 On: Thu, 27 Nov 2014 09:56:33

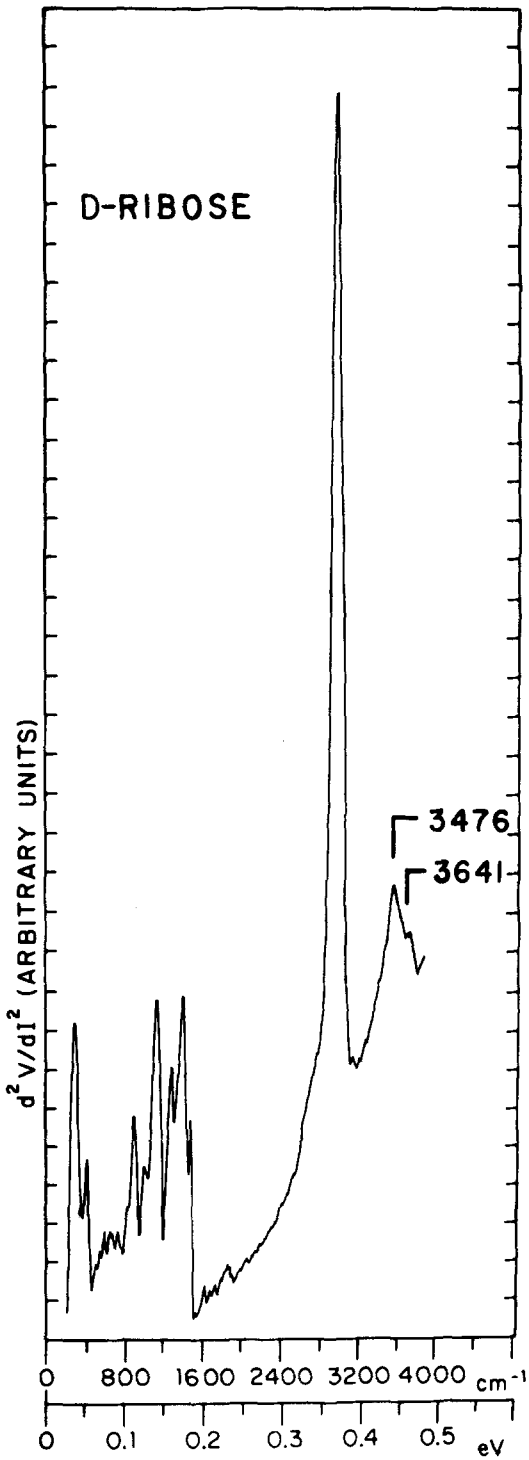

FIG. 6. IETS spectrum of *D*-ribose, 390 Ω. Spectrum was recorded at 4.2 K from an Al–AlO_x–Pb junction doped from an H_2O solution. Strong peak at 3476 cm^{-1} is due to OH group on the sugar. Shoulder at 3641 cm^{-1} is associated with the surface OH groups on the aluminum oxide.

CH_2 bending vibrations contribute in the range 1360–1460 cm^{-1} and are superimposed on the base modes in the same range. Very strong aliphatic C–H stretching modes are contributed in the range near 2900 cm^{-1}. In the absence of a detailed analysis of the vibrational motions of the sugar molecules, these assignments are transferred from spectral studies of primary and secondary alcohols and compounds containing an ether group. The IETS spectrum obtained for *D*-ribose with the junction doped and fabricated at room temperature is shown in Fig. 6. In addition to the modes below 1600 cm^{-1} already mentioned broad peaks associated with OH stretching vibrations are observed in the range 3400–3700 cm^{-1}. The maximum at 3476 cm^{-1} is identified with the OH groups on the sugar while the peak at 3641 cm^{-1} is identified with the OH groups attached to the active surface sites on the alumina due to reaction with H_2O during preparation.

In aqueous solutions of mononucleotides above *p*H 7, vibrations attributed to the phosphomonoester group $ROPO_3^{2-}$ have been observed at 980 and 1100 cm^{-1} in both Raman and infrared spectra. The strong modes in this region of the IETS spectra are present in both the nucleoside and nucleotide and are therefore not assignable to the phosphate vibrations. Since all the nucleotides examined were doped from solutions at or above *p*H 7, the absence of the modes must mean that the $-PO_3^{2-}$ moiety is protonated on the surface or has reacted with the exposed Al^{3+} ions.

IV. UV RADIATION EFFECTS

The UV radiation damage experiments are carried out by exposing the adsorbed monolayer of molecules to the direct UV beam with the substrate cooled to approximately −100 °C in a vacuum of 10^{-8} Torr. The overall features of the technique provide uniform radiation exposure to every molecule and inhibit secondary molecular changes induced by subsequent reactions in aqueous solution or atmospheres containing oxygen. The nucleotides exhibit principal absorption in the wavelength range 2400–3000 Å.[16] Wavelengths above 3000 Å are important only in photoreactivation processes which require external sensitizing agents such as dyes. Except for AMP the lowest singlet state is a $\pi\pi^*$ state which appears as a strong band in the UV absorption spectrum peaked at 2600–2800 Å. In AMP the lowest singlet state is a $n\pi^*$ state which appears slightly to the red of a strong $\pi\pi^*$ singlet band with a maximum at 2600 Å. The oscillator strengths for $\pi\pi^*$ singlet transitions are of the order of tenths.[17] The lowest triplet state for all of the nucleotides is a $\pi\pi^*$ state to which intersystem crossing takes place probably via an intermediate $n\pi^*$ triplet state. In the sugar moiety the absorption band peaks at 1800 Å in the vacuum ultraviolet.[18]

In an environment of other molecules the excited state can react by adding a water molecule across the carbon–carbon bond or similar types of attack can occur leading to saturation of the carbon–carbon bond. In the IETS experiments the alumina surface is the only source of such attack and the fixed molecular orientation and the absence of a surrounding medium during irradiation substantially reduces the reaction possibilities. The active sites on the alumina surface contain OH groups and these are potential reactants although the initial chemisorption process probably reduces their availability for subsequent reaction.

The results therefore reflect the initial primary damage to the chemical bonds of the molecule and differences in damage rates can be attributed to fundamental elec-

This article is copyrighted as indicated in the article. Reuse of AIP content is subject to the terms at: http://scitation.aip.org/termsconditions. Downloaded to IP: 128.83.63.20 On: Thu, 27 Nov 2014 09:56:33

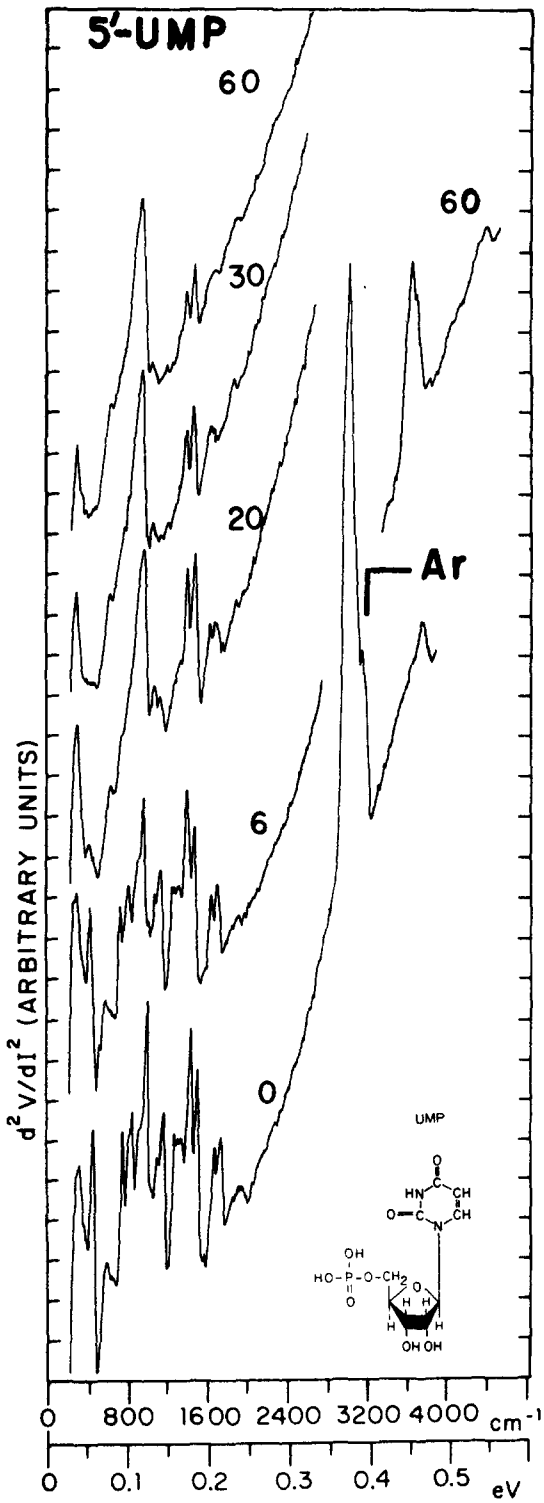

FIG. 7. UV radiation series for 5'-UMP. Time of radiation exposure in minutes is labeled for each spectrum. Spectra were recorded at 4.2 K from Al–AlO_x–Pb junctions doped from H_2O solutions. Junction substrates were held at ~ – 100 °C during irradiation and subsequent evaporation of the Pb electrode. (0) Control spectrum, 654 Ω, Ar. C–H indicates aromatic C–H stretching mode. (6) 6 min exposure, 834 Ω. (20) 20 min exposure, 468 Ω. (30) 30 min exposure, 554 Ω. (60) 60 min exposure, 52 Ω Fluence in 10 J/cm²/min equivalent to 1.26×10^3 photons/Å²/min at an average wavelength of 2500 Å.

tronic differences in the bond structure and cross sections. The detailed analysis of the experimental environment and the role of the surface adsorption will be discussed more fully in Sec. V. The results so far obtained are most detailed for the nucleotide components of RNA however results on 5'-dAMP and 5'-dTMP have

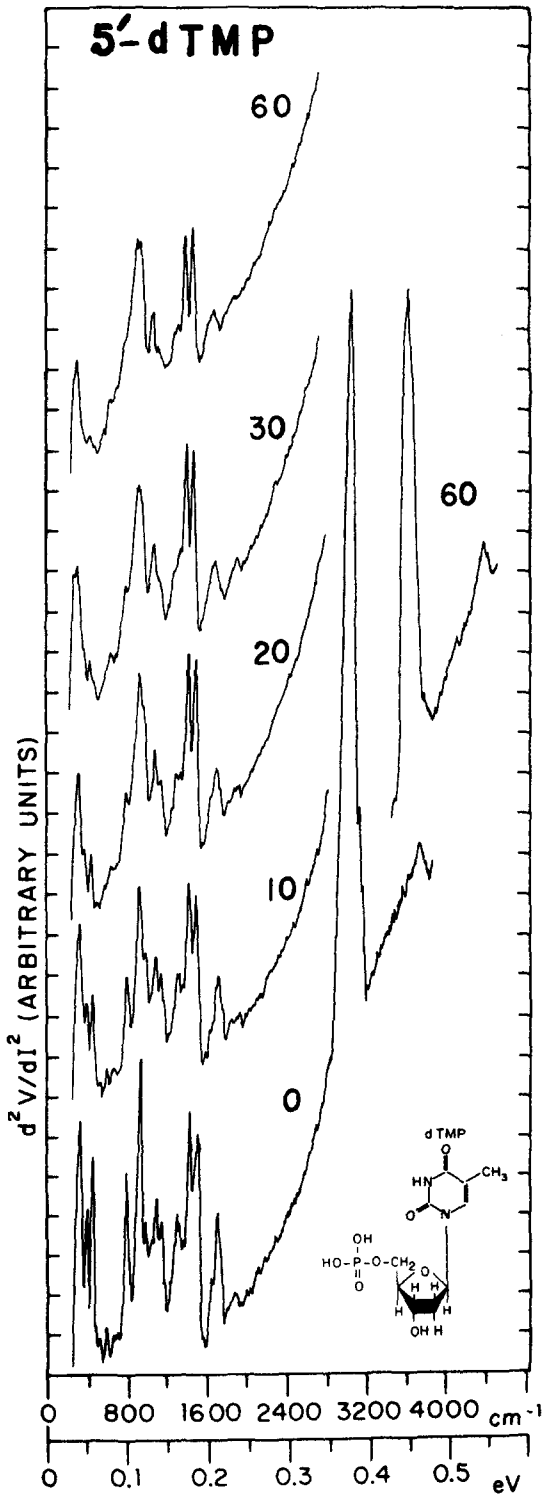

FIG. 8. UV radiation series for 5'-dTMP. Junction substrates were held at ~ – 100 °C during irradiation and evaporation of the Pb electrode. Spectra were recorded at 4.2 K from Al–AlO_x–Pb junctions doped from H_2O solutions. (0) control spectrum, 407 Ω. (10) 10 min exposure, 734 Ω (20) 20 min exposure, 263 Ω. (30) 30 min exposure, 436 Ω. (60) 60 min exposure, 150 Ω. Fluence is 10 J/cm²/min.

This article is copyrighted as indicated in the article. Reuse of AIP content is subject to the terms at: http://scitation.aip.org/termsconditions. Downloaded to IP: 128.83.63.20 On: Thu, 27 Nov 2014 09:56:33

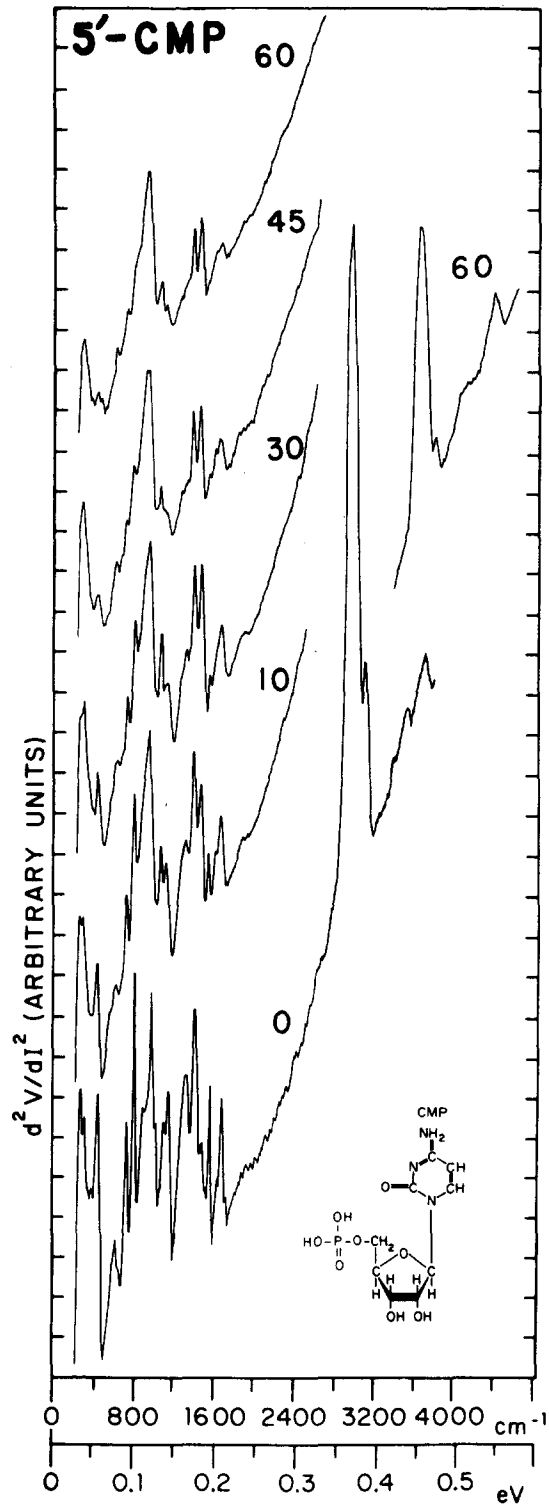

FIG. 9. UV radiation series for 5'-CMP. Junction substrates were held at ~ −100°C during irradiation and evaporation of the Pb electrode. Spectra were recorded at 4.2 K from junctions doped from H_2O solutions. (0) Control spectrum, 450 Ω. (10) 10 min exposure, 166 Ω (30) 30 min exposure, 117 Ω. (45) 45 min exposure, 160 Ω. (60) 60 min exposure, 90 Ω. Fluence is 10 J/cm^2/min.

also been obtained. Selected results on individual bases, on *D*-ribose and on peptide chains will also be summarized.

A. Nucleotides

Figures 7, 8, and 9 show the sequence of IETS spectra obtained for UV radiation damage to 5'-UMP, 5'-dTMP, and 5'-CMP for exposure times ranging from 0 (control) to 60 min. The sequence of spectra shown in the figures include the C–H stretching mode region only for the 0 and 60 min irradiations. The C–H stretching region is detached and moved to the right for the 60 min spectrum represented by the top curve in the figures.

The three nucleotides 5'-UMP, 5'-dTMP, and 5'-CMP all develop UV damage at comparable radiation levels and show generally the same type of damage. As UV exposure time is increased selected peaks show a substantial reduction in intensity. Particularly strong reductions occur for the peaks assigned to base ring modes and to out of plane C–H bending modes as identified in Sec. III A. The ring mode near 430 cm^{-1} shows a large reduction in intensity for all three compounds and this loss of skeletal vibration intensity indicates a disruption of the pyrimidine ring in the initial stage of the damage sequence. The C=C and C=O bonds to not appear to damage at the same rate. The final radiation product (60 min exposure) is basically the same for all three compounds. The prominent features are the strong, broad peak centered at 930 cm^{-1}, a mode at 1060 cm^{-1}, sharp peaks at 1380 and 1450 cm^{-1} and a strong peak near 2900 cm^{-1}. The peak at 930 cm^{-1} is the alumina mode; the remaining peaks correspond to rocking, and in plane bending and stretching modes of CH and CH_2 groups. These vibrations would be expected to characterize radiation fragments. The aromatic C–H stretching vibration seen as a side-peak or shoulder at 3050 cm^{-1} in the control spectra labeled Ar in Fig. 7 has been quenched in UMP and dTMP and almost quenched in CMP after irradiation. The peak at 300 cm^{-1} is a phonon mode of the aluminum electrode. A major reduction in mode intensity is also observed in the UMP spectrum for modes at 726, 786, 811, and 1117 cm^{-1}; in the dTMP spectrum for modes at 375, 766, and 1117 cm^{-1}; and in the CMP spectrum for modes at 726, 794, 1125, 1294, and 1536 cm^{-1}.

As shown in Figs. 10 and 11, 5'-AMP and 5'-GMP do not damage as easily as the nucleotides containing the pyrimidine bases. After a 30 min exposure the spectrum of AMP is not appreciably different from the control spectrum. However, spectral modifications are evident after a 50 min dose; the region 800–1000 cm^{-1} is more diffuse and the region 1300–1500 cm^{-1} is dominated by twin peaks at 1380 and 1460 cm^{-1} just as in the case of the pyrimidine nucleotides. The strong ring deformation mode at 690 cm^{-1} is depressed quite rapidly, but is still evident after a 50 min UV exposure. In GMP the onset of damage is more rapid, as evidenced by the formation of these same spectral features after only a 20–30 min dose. The 698 cm^{-1} mode assigned to the guanine ring damages fairly rapidly but is still discernible after 50 min exposure.

In both purine nucleotides the primary UV damage is again assignable to disruption of the internal base ring modes with less initial damage to the double bond structure. In fact for the AMP damage sequence the forma-

This article is copyrighted as indicated in the article. Reuse of AIP content is subject to the terms at: http://scitation.aip.org/termsconditions. Downloaded to IP: 128.83.63.20 On: Thu, 27 Nov 2014 09:56:33

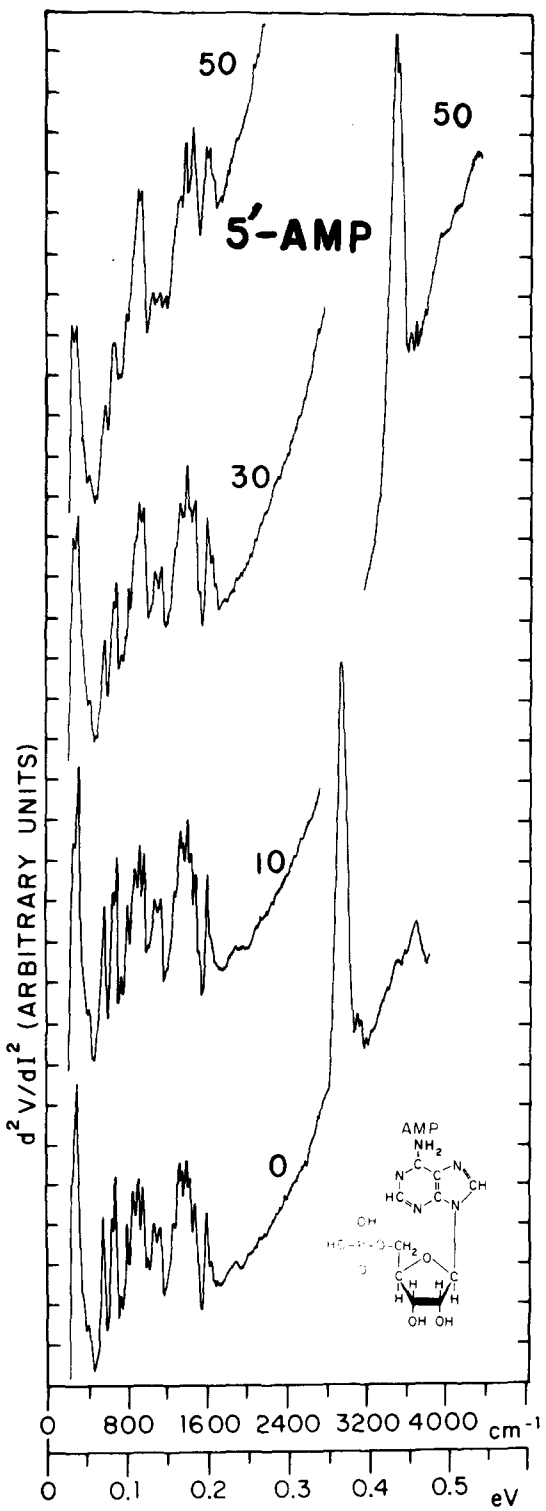

FIG. 10. UV radiation series for 5'-amp. Ring modes are more resistant to damage than for the pyrimidine base nucleotides and double bond structure near 1600 cm^{-1} increases during UV exposure (see Fig. 12). Junction substrates were held at ~ – 100 °C during irradiation and evaporation of the lead electrode. Spectra were recorded at 4.2 K from junctions doped with H_2O solutions. (0) Control spectrum, 331 Ω. (10) 10 min exposure, 447 Ω. (30) 30 min exposure, 744 Ω. (50) 50 min exposure, 365 Ω. Fluence is 10 J/cm^2/min.

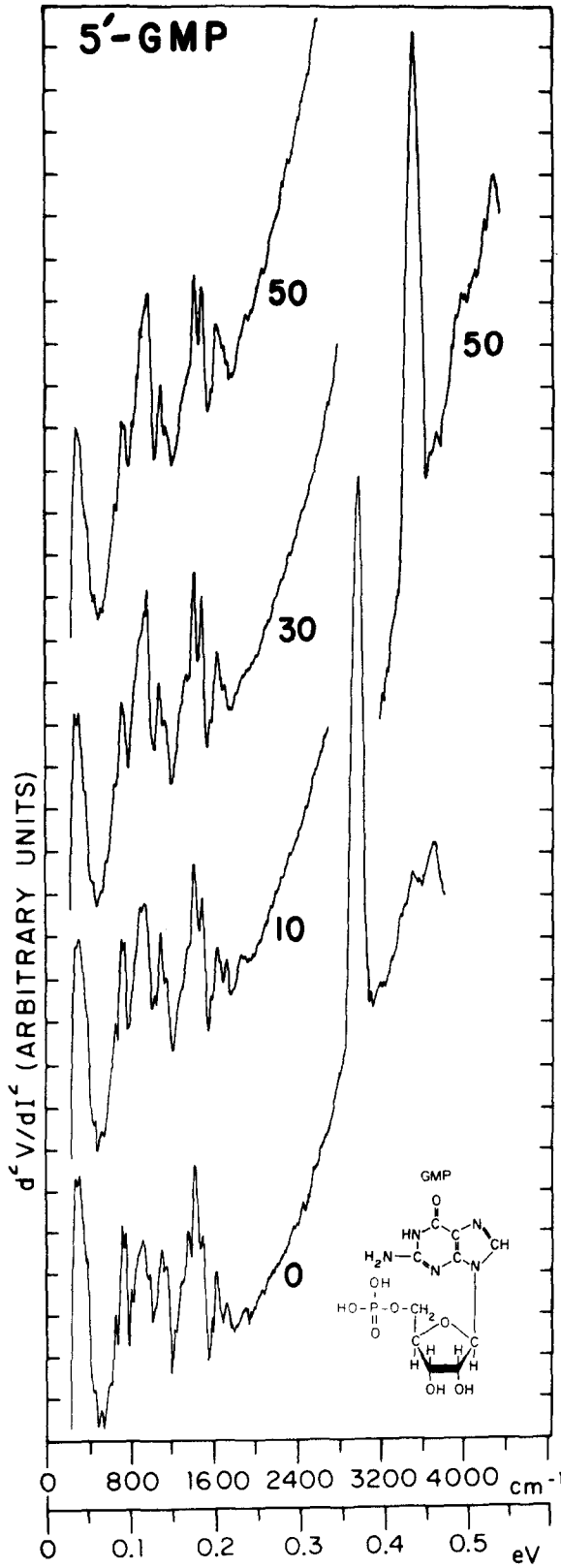

FIG. 11. UV radiation series for 5'-GMP. Junction substrates were held at ~ – 100 °C during irradiation and evaporation of the lead electrode. Spectra were recorded at 4.2 K from junctions doped from H_2O solutions. (0) Control spectrum, 1120 Ω. (10) 10 min exposure, 410 Ω. (30) 30 min exposure, 366 Ω. (50) 50 min exposure, 1390 Ω. Double bond structure just above 1600 cm^{-1} also increases during UV exposure. Fluence is 10 J/cm^2/min.

tion of what appear to be additional double bond modes above 1600 cm^{-1} is observed. These modes are identi-

This article is copyrighted as indicated in the article. Reuse of AIP content is subject to the terms at: http://scitation.aip.org/termsconditions. Downloaded to IP: 128.83.63.20 On: Thu, 27 Nov 2014 09:56:33

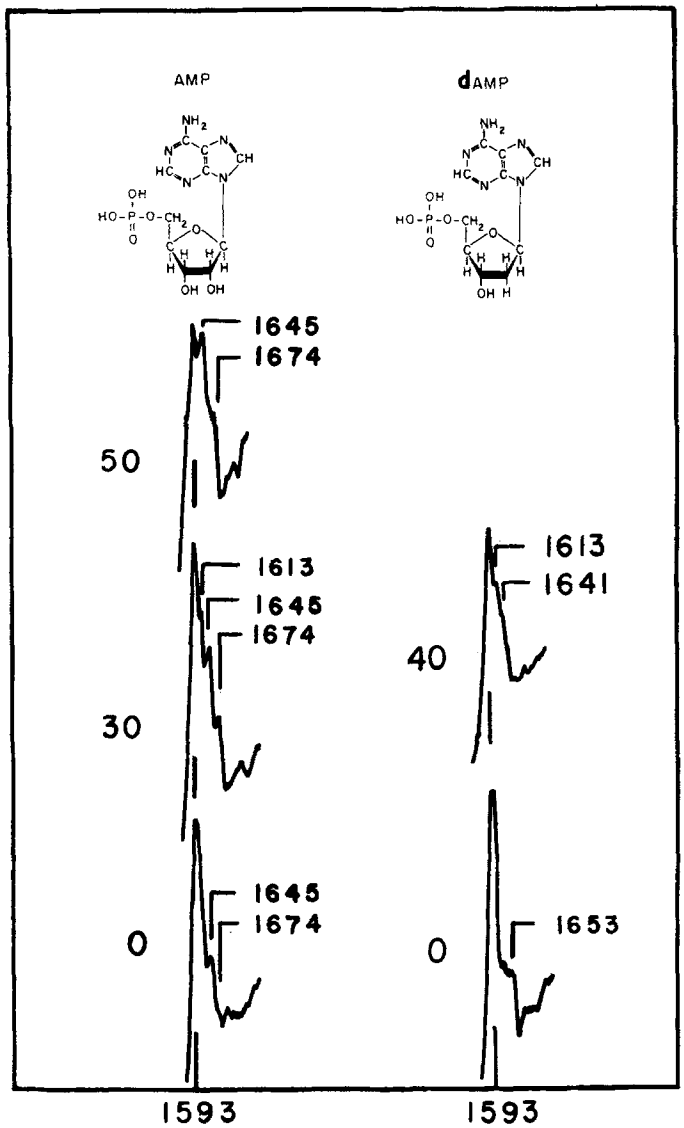

FIG. 12. Detail of vibrational mode development in 5′-AMP and 5′-dAMP during UV radiation exposure. A strong stable mode is observed at 1593 cm^{-1} in both nucleotides while new modes develop at 1613 and 1674 cm^{-1} in 5′-AMP and at 1613 cm^{-1} in 5′-dAMP. A mode at 1645 cm^{-1} weakly present in the unirradiated spectrum develops additional intensity during irradiation. Spectra shown are from narrow range of complete spectra shown in Figs. 10 and 13.

fied in Fig. 12 where a magnified portion of the AMP spectrum in the relevant frequency range is shown. In the control spectrum of AMP (0 min), a peak at 1593 cm^{-1} attributed to coupled C=C and C=N vibrations and a peak at 1633 cm^{-1} attributed to an NH_2 scissoring vibration are present. As the UV exposure is increased, the mode at 1593 cm^{-1} is stable both in frequency and intensity, and new peaks appear at 1645 and 1674 cm^{-1} both of which become more intense. A shoulder peak at 1613 cm^{-1} can also be seen after a 30 min dose, but at higher doses the peak is masked by the mode at 1645 cm^{-1}. The peak at 1674 cm^{-1} occurs at a frequency characteristic of C=O or possibly C=C bonds.

The substitution of 2-deoxy-*D*-ribose for *D*-ribose in 5′-AMP to form 5′-dAMP does not alter the damage sequence of AMP except in the double bond stretching region, which in this case shows no mode at 1674 cm^{-1}. The tunneling spectra of dAMP irradiated for 0 and 40 min are shown in Fig. 13 while the double bond stretch region has again been emphasized in Fig. 12. In the control spectrum of dAMP (0 min) modes are present at 1593 and 1653 cm^{-1}; in the spectrum of radiated dAMP, modes are present at 1593, 1613, and 1641 cm^{-1}. The mode at 1593 cm^{-1} is relatively stable while the mode at 1641 cm^{-1} shows a clear intensity enhancement at higher exposure. In the radiation series for GMP (Fig. 11) the growth of additional double bond modes is not as evident as in AMP, but a similar trend is observed. For example a new mode at 1660 cm^{-1} is definitely resolved and is identified in the 60 min exposure of Fig. 11.

The spectra of pyrimidine nucleotides exposed to large doses of ultraviolet radiation (Figs. 7–9) are dominated by the bending and stretching vibrations of CH and CH_2 groups and by strong alumina phonon modes. The peaks at 1380 and 1450–1560 cm^{-1} can be assigned to bending vibrations (the latter a CH_2 bending mode) and the strong peak at 2900 cm^{-1} to the aliphatic C–H stretching mode. The weaker peak at 1060 cm^{-1} is thought to arise from a bending vibration of CH bonds reacted with sites on the alumina surface. The purine nucleotides were not radiated to the point of complete degradation, but the development of these same peaks is evident in their spectra at higher exposures. The final products of the UV irradiation of both pyrimidine and purine nucleotides are consistent with saturated CH fragments formed from the sugar and aromatic rings.

B. Bases

In contrast to other base residues relatively high resistance junctions can be obtained with cytosine doped from solution at room temperature. This has allowed us to carry out a UV radiation sequence and to compare the results with those obtained for the corresponding nucleotide CMP. The spectrum of cytosine irradiated for 40 min as shown in Fig. 14 displays structural damage which, unlike CMP, is selective. This can be seen by carefully comparing the modes in the spectrum of irradiated cytosine with the modes in the control spectrum. Peaks at 726 and 799 cm^{-1} are fairly intense even after a 40 min dose while peaks at 1290 and 1528 cm^{-1} are quenched. The sharp peak at 432 cm^{-1} shows a significant reduction. All of these modes, except the 726 cm^{-1} mode, were assigned ring character in Sec. III A. The presence of a strong aromatic C–H stretching mode at 3045 cm^{-1} in the spectrum of irradiated cytosine is an indication that the π electron system of the ring is relatively resistant to damage. A final point to notice is that the cytosine base is considerably more resistant to ultraviolet radiation than the corresponding nucleotide. This can be seen by comparing the spectrum of irradiated cytosine in Fig. 14 with that of CMP at approximately equal exposure as shown in Fig. 9. A number of IETS studies[7] have shown that ring compounds with substituted groups that act as proton donors to the alumina surface can enhance the intensity of the tunneling spec-

This article is copyrighted as indicated in the article. Reuse of AIP content is subject to the terms at: http://scitation.aip.org/termsconditions. Downloaded to IP: 128.83.63.20 On: Thu, 27 Nov 2014 09:56:33

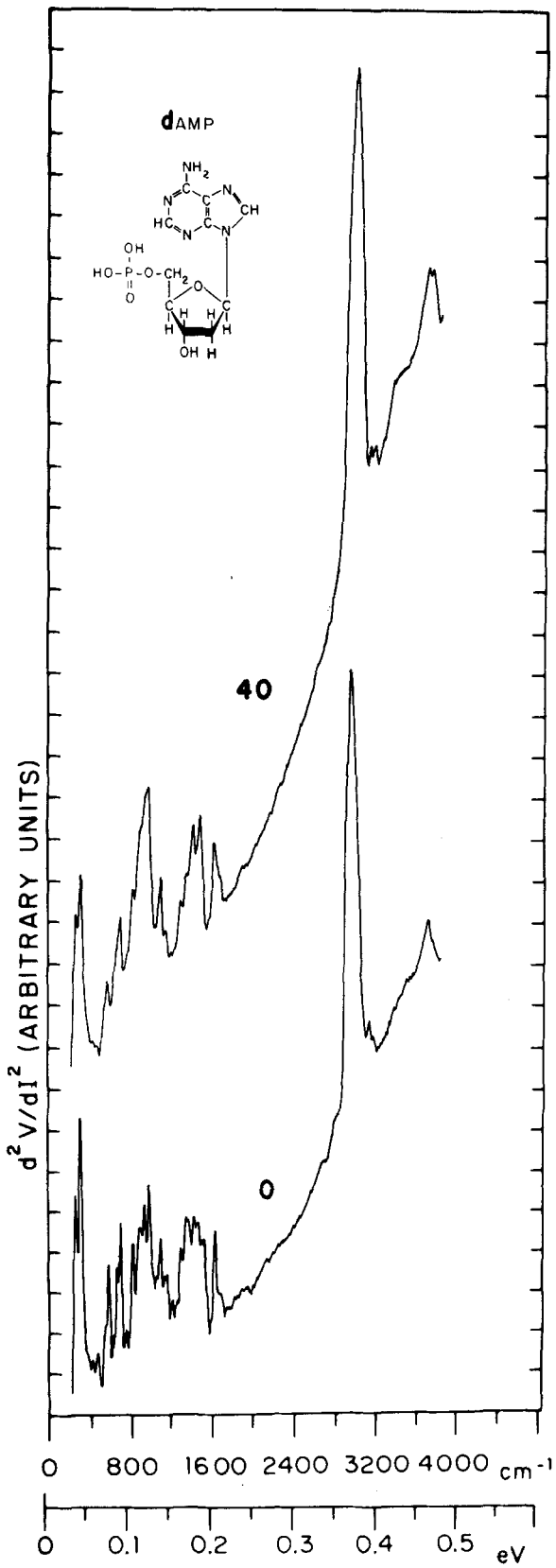

FIG. 13. UV radiation of 5′-dAMP. (0) Control spectrum, 375 Ω. (40) 40 min exposure, 275 Ω. The spectral changes during irradiation are similar to those observed in 5′-AMP except for slight differences in the development of the double bond intensity near 1600 cm^{-1} (see also Fig. 12).

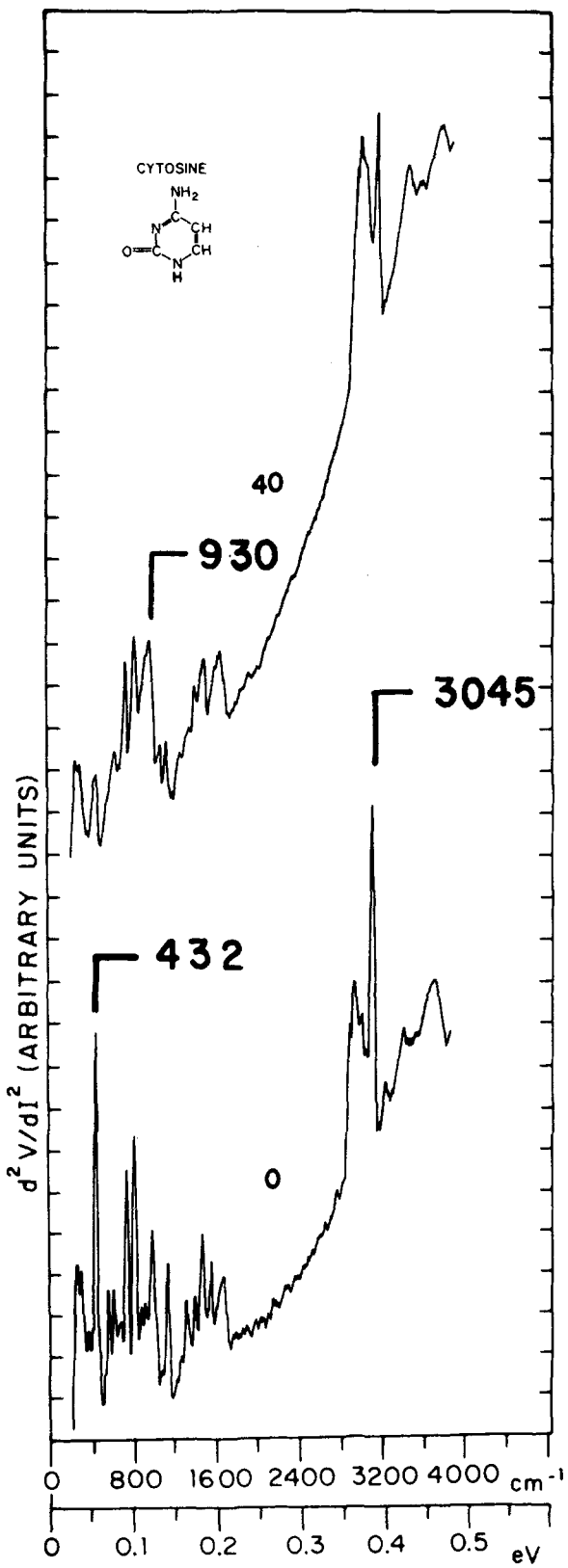

FIG. 14. UV radiation of cytosine. (0) Control spectrum, 505 Ω. (40) 40 min exposure, 222 Ω. Spectra were recorded at 4.2 K from Al–AlO_x–Pb junctions doped from H_2O solutions. The sharp peak at 432 cm^{-1} identified with a ring deformation mode is rapidly reduced in intensity. A surface phonon mode of the aluminum oxide near 930 cm^{-1} is enhanced by the UV exposure. The aromatic D–H stretching mode at 3045 cm^{-1} and the asymmetric N–H stretching mode at 3351 cm^{-1} are only partially reduced by UV exposure.

This article is copyrighted as indicated in the article. Reuse of AIP content is subject to the terms at: http://scitation.aip.org/termsconditions. Downloaded to IP: 128.83.63.20 On: Thu, 27 Nov 2014 09:56:33

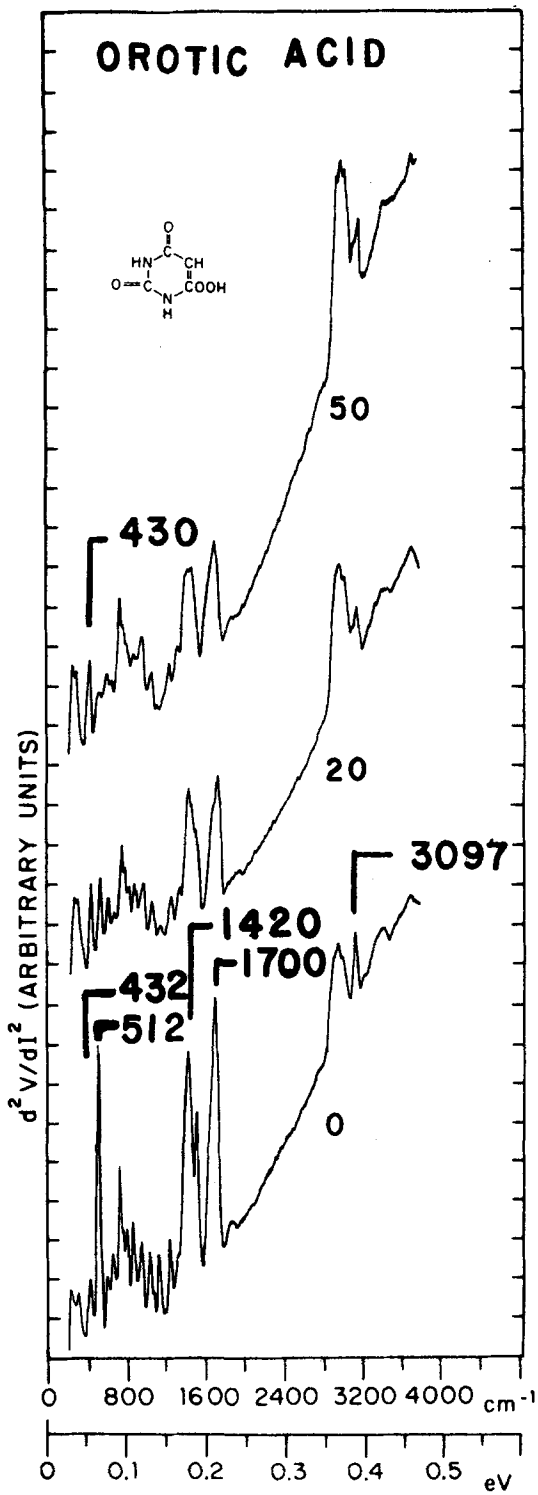

FIG. 15. UV radiation of orotic acid (6-methyluracil). (0) Control spectrum, 243 Ω. (20) 20 min exposure, 184 Ω. (50) 50 min exposure, 225 Ω. Spectra were recorded at 4.2 K from Al–AlO_x–Pb junctions doped from H_2O solutions. COHH group adsorbs on the alumina as a CO_2^- ion with a symmetric bidentate structure. Symmetric stretching mode of the CO_2^- is the strong mode at 1420 cm^{-1}. Ring deformation mode at 512 cm^{-1} is rapidly quenched by UV exposure. The mode at 430 cm^{-1} increases in intensity during UV exposure. The relative strength of the carbonyl C=O stretch modes at 1700 cm^{-1} and the aromatic C–H stretching mode at 3097 cm^{-1} remain strong during irradiation and indicates that the ring structure persists during UV exposure.

trum. For example the COOH group on benzoic acid or on *L*-phenylalanine donates a proton and forms a monocarboxylate anion with a symmetric bidentate structure bonded to the alumina surface. Although this bonding structure leaves the molecule free to cant it probably maintains the ring at an appreciable angle to the surface. The IETS vibrational modes agree well with the Raman or infrared modes of the free carboxylate ion. These are very similar to the neutral molecule modes except for the strong distinct modes associated with the symmetric and asymmetric stretching modes of the CO_2^- ion observed in the ranges 1420 to 1460 cm^{-1} and 1560–1580 cm^{-1}, respectively.

Substitution of a carboxyl group at position 6 on the uracil ring (orotic acid) induces a greater adsorption on the alumina substrate and the IETS intensity is also enhanced particularly for the symmetric carboxylate mode at 1420 cm^{-1} and for the carbonyl (C=O) stretch modes near 1700 cm^{-1} as shown in Fig. 15. The partial lifting of the ring due to the surface bonding of the COOH substituent changes the relative proximity of the carbonyl groups to the surface and allows them to couple more effectively to the tunneling electron. There may also be some subtle shift in the π electron interaction with the surface.

The stronger binding to the alumina surface allows the fabrication of higher resistance junctions which are well suited to UV radiation studies. Figure 15 shows IETS spectra for UV exposures of 20 and 50 min. The peaks at 512, 863, and 1125 cm^{-1} are quite sensitive to UV radiation and lose intensity rapidly as compared to the other modes. In contrast the intensity of the mode at 430 cm^{-1} increases by almost a factor of 2 after a 50 min exposure. The very strong mode at 512 cm^{-1} is identified with a ring deformation mode which is observed at 432 cm^{-1} in pure uracil and is shifted up by the COOH substitution and surface bonding. It damages rapidly as was also observed for this mode in cytosine as demonstrated in Fig. 14.

For the C–H stretching modes near 3000 cm^{-1} the UV exposure produces an increase in the aliphatic C–H component and a decrease in the aromatic C–H component. This follows the general trend for the other compounds where radiation products are CH fragments which are relatively less sensitive to UV damage. As in the case of cytosine the isolated base structure is not as sensitive to UV damage as is the corresponding nucleotide.

In contrast to cytosine and to the nucleotide IETS spectra continued UV exposure of orotic acid does not enhance and broaden the aluminum oxide phonon modes at 930 cm^{-1}. This strong enhancement was identified in the cytosine spectrum of Fig. 14. The strong surface binding and specific surface structure of the CO_2^- group on the alumina surface may prevent modification of the surface phonons by the UV radiation. In the case of compounds with weaker and less specific bonding the surface site structure involving OH groups can be more sensitive to modification by UV radiation. The other base residues can probably be studied under UV radiation using IETS but will require special doping techniques and further development.

This article is copyrighted as indicated in the article. Reuse of AIP content is subject to the terms at: http://scitation.aip.org/termsconditions. Downloaded to IP: 128.83.63.20 On: Thu, 27 Nov 2014 09:56:33

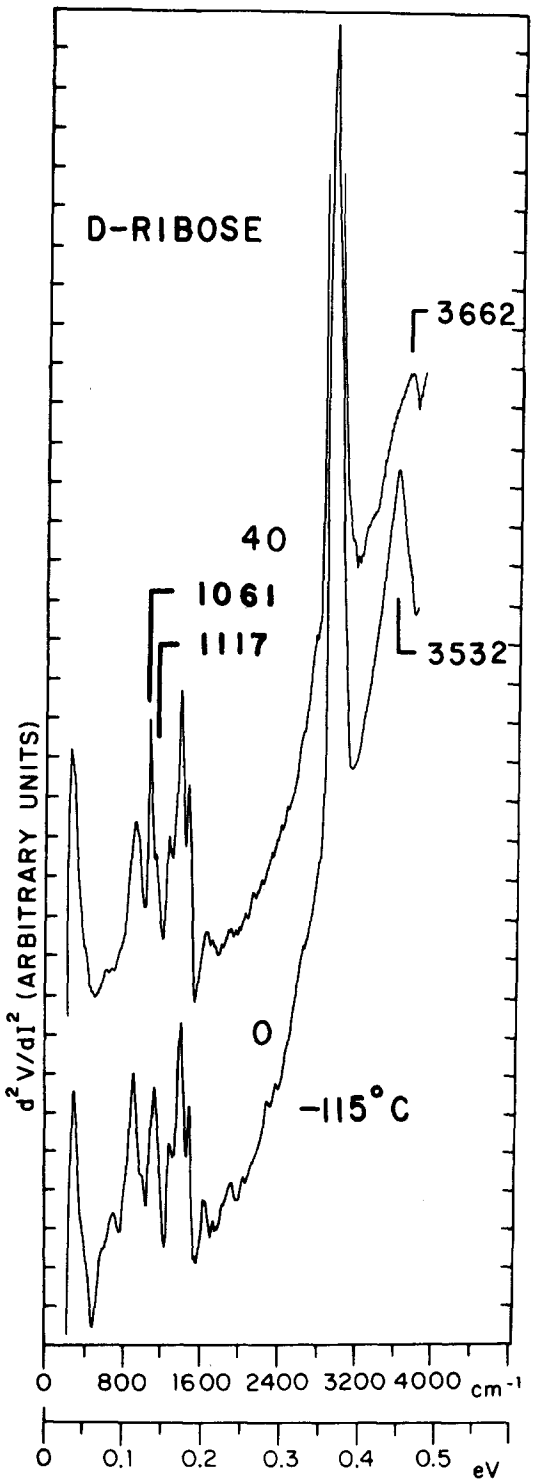

FIG. 16. UV radiation of *D*-ribose. (0) Control spectrum with substrate cooled to −115 °C during evaporation of the Pb electrode, 1557 Ω. (40) 40 min exposure, 400 Ω. Spectra were recorded at 4.2 K from Al–AlO_x–Pb junctions doped from H_2O solutions. The UV radiation splits the peak near 1100 cm^{-1} into a strong sharp peak at 1061 cm^{-1} and a weak shoulder at 1117 cm^{-1}. For the control spectrum substrate cooling during Pb evaporation has reduced the low lying ring mode intensity and downshifted the surface O–H stretching mode to 3532 cm^{-1} as compared to the Pb evaporation at room temperature (see Fig. 6). The UV exposure before Pb evaporation reshifts the surface O–H stretching mode to 3662 cm^{-1} which is approximately the room temperature position.

C. *D*-ribose

The control spectrum and a spectrum obtained after a 40 min UV radiation of *D*-ribose are shown in Fig. 16. The spectrum of *D*-ribose irradiated for 40 min shows little overall decrease in intensity except for the peak at 1100 cm^{-1} and the OH peak at 3532 cm^{-1}. The effect of UV is to split the peak at 1100 cm^{-1} into a strong sharp peak at 1061 cm^{-1} and a weak shoulder at 1117 cm^{-1}. An identical effect is observed when β-*D*-fructose, a molecule similar in structure to *D*-ribose, is radiated with energetic electrons.[3] The C–O stretching vibrations of primary and secondary alcohols are known to occur near 1050 and 1100 cm^{-1}, respectively. The C–O–C stretch mode in cyclic ethers is expected near 1070 cm^{-1}. The loss of intensity at 1117 cm^{-1} and the accompanying depletion of the OH stretch modes of the sugar molecule indicate that the hydroxyl groups, probably at the 2′ and 3′ sites, are disrupted by the action of UV. The CH and CH_2 groups of the molecule exhibit a high resistance to ultraviolet radiation while the C–OH functional groups show a much lower resistance.

In using the IETS technique for a wide range of organic compounds it has been found that cooling the substrate before the lead evaporation can alter the spectrum of some compounds. This effect is much stronger in some compounds than in others and is definitely correlated with the initial chemisorption process for the particular molecule. No effects of this sort were observed for the nucleotides, however the isolated *D*-ribose molecule shows some modification which can be seen by comparing the control spectrum of Fig. 16 (cooled to −115 °C) with the room temperature spectrum of Fig. 6. The major changes are observed below 1000 cm^{-1} while the modes of the CH and C–OH functional groups above 1000 cm^{-1} shows only small variations in relative intensity. Ring modes below 800 cm^{-1} are substantially reduced in intensity by substrate cooling. In addition the surface OH modes are downshifted during cooling and the relevant modes have been labeled in Figs. 6 and 15. In the room temperature spectrum, the peak at 3641 cm^{-1} is the stretching vibration of the surface OH groups; the stronger peak at 3476 cm^{-1} is the stretching vibration of the hydroxyl groups of the sugar molecule. When the substrate is cooled, the surface modes shift down in frequency so that only one peak is observed with a centroid at 3532 cm^{-1}. The cooling should not affect the chemical structure of the sugar molecule but does affect the detailed surface adsorption structure.

The point to be emphasized with regard to the IETS radiation technique is that whenever the substrate is cooled to sufficiently low temperature, it is necessary to use the cooled control spectrum as the baseline for radiation data interpretation of a given molecule since it may differ from the room temperature spectrum. We emphasize again however, that for nucleotides this is not necessary since the specific geometry of the base and sugar rings apparently stops the temperature dependent surface reaction that is observed for planar ring compounds.

This article is copyrighted as indicated in the article. Reuse of AIP content is subject to the terms at: http://scitation.aip.org/termsconditions. Downloaded to IP: 128.83.63.20 On: Thu, 27 Nov 2014 09:56:33

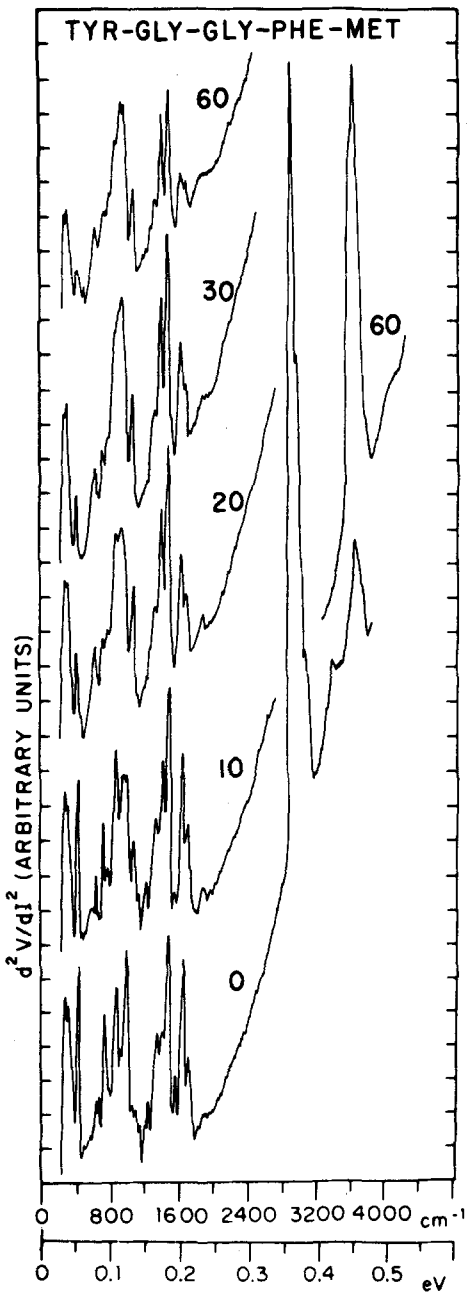

FIG. 17. UV radiation series for polypeptide tyrosine–glycine–phenylalanine–methionine. (0) Control spectrum, 166 Ω. (10) 10 glycine–min exposure, 235 Ω. (20) 20 min exposure, 69 Ω. (30) 30 min. exposure, 92 Ω. (60) 60 min exposure, 40 Ω. Spectra were recorded at 4.2 K from Al–AlO_x–Pb junctions doped from H_2O solutions. Final damage spectrum (60 min) shows a strong alumina phonon mode structure and strong C–H bending modes similar to the final products observed for the pyrimidine nucleotides.

D. Peptide chains and surface reactions

Preliminary results on UV damage to polypeptide chains have been obtained using the IETS technique. These chains of amino acids show damage rates comparable to the more easily damaged nucleotides although a detailed analysis of the difference between the ring and straight chain segments has not been made. An example for a five component polypeptide is shown in Fig. 17. The final IETS spectrum obtained after a 60 min UV exposure shows strong alumina phonon modes and C–H bending modes similar to those which develop for the pyrimidine nucleotides (see dTMP, Fig. 8) which also show fairly rapid UV damage. The C–H bending modes above 1400 cm^{-1} are very strong throughout the UV exposure while ring modes and combination modes at lower wave numbers damage rapidly.

In contrast to the nucleotides the surface interaction of the polypeptides is temperature dependent and this must be considered in evaluating the control spectrum. An example of the temperature induced change in the IETS spectrum is shown for the dipeptide *L*-tryptophyl-*L*-phenylalanine in Fig. 18(a). At 22 °C the IETS spectrum exhibits very strong modes as shown in the lowest curve of Fig. 18(a). Most of the ring modes are nearly quenched by cooling the substrate to −115 °C before evaporating the lead electrode as shown in the upper curve of Fig. 18(a). Evaporation of the lead electrode freezes the spectral intensity characteristic of the substrate temperature at the time of evaporation. Before evaporation of the lead electrode the intensity changes and OH frequency shift are completely reversible as demonstrated for temperature cycling in the middle spectrum of Fig. 18(a).

The effects of substrate cooling on the IETS spectra are associated with the surface reaction of the molecule and the active binding sites on the surface. Possible changes in OH adsorption and interchange of molecular groups at the adsorption sites may also play some role. For the spectrum obtained with the substrate cooled to −115 °C the surface alumina phonons in the range 900–1000 cm^{-1} show large relative intensity enhancement and the surface OH stretching mode has downshifted by over 100 cm^{-1}. The adsorbed molecular configuration in the case of polypeptides is apparently much less constrained than is the case of nucleotides and the substrate temperature reduction can produce a much greater change in electron–phonon coupling. These effects show rapid changes near −100 °C and for the most sensitive molecules the control spectrum and irradiated spectra should be held above this temperature when depositing the lead electrode.

Figure 18(b) shows a comparison of the tunneling spectrum obtained for a CMP junction prepared with the substrate at room temperature and cooled to −115 °C. The spectra are essentially identical and no downshift of the OH stretching mode is observed for the cooled substrate in this case.

V. DISCUSSION

A. Effects of surface chemisorption and IETS methods on UV damage

The techniques used for these experiments present a unique combination of surface–molecular–photon interaction. The role of the surface involves both the orientation and the initial chemical reaction of the molecule with the surface as well as the effect of the surface on possible secondary reactions of products following irradiation.

This article is copyrighted as indicated in the article. Reuse of AIP content is subject to the terms at: http://scitation.aip.org/termsconditions. Downloaded to IP: 128.83.63.20 On: Thu, 27 Nov 2014 09:56:33

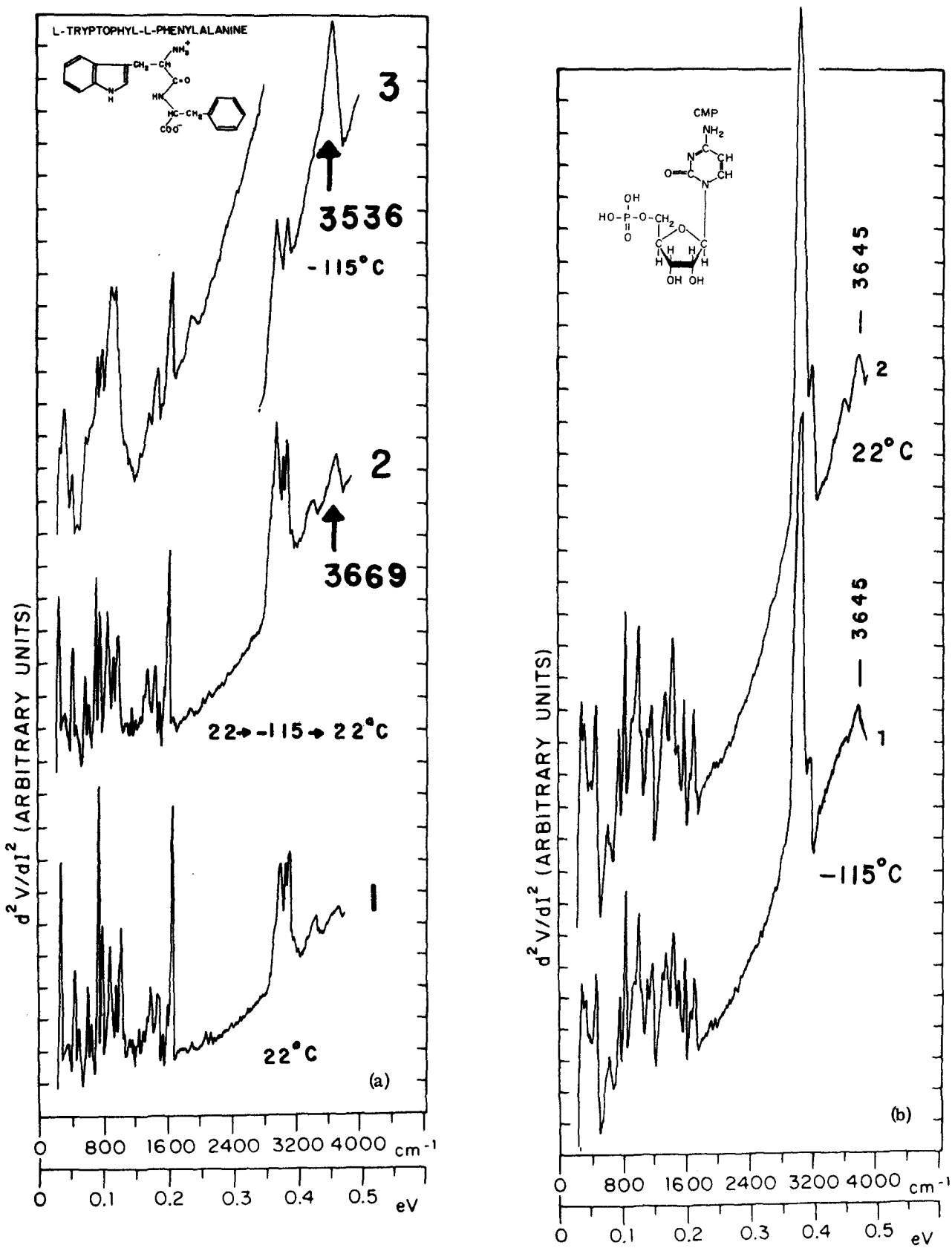

FIG. 18. (a) IETS spectra of the dipeptide *L*-tryptophyl-*L*-phenylanine. (1) Spectrum obtained after evaporation of the Pb electrode at 22°C, 810 Ω. (2) Doped substrate cooled to −115°C and then reheated to 22°C before evaporation of the Pb electrode, 258 Ω. (3) Doped substrate cooled to −115°C before evaporation of the Pb electrode, 270 Ω. This spectrum shows a reduced ring mode intensity and an enhanced and downshifted surface O–H stretching mode at 3536 cm^{-1}. All spectra were recorded at 4.2 K from Al–AlO_x–Pb junctions doped from a solution of peptide, NH_4OH, and H_2O. (b) IETS spectra of 5′-CMP obtained with Pb electrode evaporated at −115°C (1) and at 22°C (2). The two spectra are nearly identical with no downshift of the OH mode and no intensity reduction for the cooled substrate.

This article is copyrighted as indicated in the article. Reuse of AIP content is subject to the terms at: http://scitation.aip.org/termsconditions. Downloaded to IP: 128.83.63.20 On: Thu, 27 Nov 2014 09:56:33

From the standpoint of surface adsorption on alumina the IETS spectra of the nucleotides show several important characteristics. As previously mentioned the IETS mode frequencies are in good agreement with Raman studies and the most intense low lying modes are identified with the base ring as is also the case for Raman spectra. Similar relative and absolute mode intensities are observed in IETS for all of the nucleotides studied so far and we conclude that the surface reaction and general conformation of the molecule is the same in all cases. The most likely adsorption interaction sites on the nucleotide are the base ring nitrogen and possibly the oxygen ring substituent as well as the phosphomonoester group on the sugar. The absence of modes associated with the phosphomonoester group suggests that it reacts with the surface and this will inhibit participation of this group in secondary reactions following irradiation.

As previously pointed out the presence of the sugar–phosphate moieties on the base increase the chemisorption on the alumina substrate and an ideal range of reproducible tunnel junction resistance can be obtained. Although a sufficient chemisorption is obtained no strong modifications of the spectra occur due to substrate cooling or to variations in substituents and bases. In contrast polypeptides as well as selected single and multiple aromatic ring compounds can show strong IETS mode reductions when adsorbed on the alumina substrate or when the substrate is cooled below room temperature.[18] In reference to Fig. 18(a) it was pointed out that a cooled substrate can greatly reduce the ring mode intensity while structure due to the alumina surface and adsorbed OH become enhanced. This may result from surface displacement by molecular fragments or by additional adsorption of H_2O. The complete reversibility of the effect which is obtained on reheating the substrate indicates that the adsorbed molecules undergo no permanent change. The loss of IETS intensity may be due to subtle electronic changes in the adsorbed molecular layer or to interference with the tunneling electron coupling due to additional adsorbed water. The degree to which the IETS spectrum is affected by substrate temperature is directly correlated with the strength of the chemical binding to the alumina substrate, but even strong binding compounds can be modified at sufficiently low temperatures.

The resistance of the adsorbed nucleotides to such effects is at present not precisely understood. The base and sugar rings connected by the glycosidic bond form a complex which may limit surface interaction and fix the relative orientation of the rings relative to the surface. Various studies involving x-ray diffraction and other methods[19] show that the sugar ring can rotate about the glycosidic bond and can assume either of two positions relative to the base approximately 150° apart. At either of these positions the relative sugar position can change within a ~45° range in response to interactions with the base ring. Precise details of the axes used to define the angles and the relative orientations of the ring planes can be found in Ref. 19. In general the two planes will be held at a reasonably large angle to each other and the complex should orient on the alumina surface with both rings off the surface which probably limits further surface interaction.

In considering all of the above observations we conclude that the experiment provides approximately a monolayer of nucleotide molecules oriented relative to the surface and all of them receive an equal dose of UV radiation. The surface chemisorption does not perturb the molecule significantly but limits any secondary reaction of the excited states or radiation products. Evaporation of the lead electrode following the irradiation is carried out without breaking vacuum and shields the radiation products from oxygen when the junction is afterwards exposed to air. Irradiated compounds which might further react with their surroundings and spontaneously revert to the original undamaged state after short periods of time (minutes) are thus shielded from such reactions by the junction fabrication used in the tunneling technique.

B. Interpretation of UV damage to nucleotides

The IETS data on UV radiation damage shows a substantial variation in damage rate for nucleotides containing different base residues. These differences have been estimated by comparing the decrease in selected mode intensity as a function of radiation exposure time. For the most sensitive low lying ring mode identified as a ring deformation mode the damage rate has been observed to vary by at least a factor of 5. The relative order of the damage rates observed for the various nucleotides is listed as follows and generally holds for all of the strong ring modes measured:

$$\text{UMP} > \text{dTMP} > \text{CMP} > \text{GMP} > \text{AMP}\ .$$

UMP is the most sensitive to UV radiation while AMP is the least sensitive. The relative order of radiation resistance observed for the nucleotides is correlated with the relative stability of the base residues as measured by the delocalization energy per π electron.[20] The higher resonance energy implies a greater delocalization of the π electrons and a higher probability of converting excitation energy into nondissociative channels. The calculated resonance energies for the ground and first excited states of the purine and pyrimidine bases are listed in Table VI and follow the same order as observed for the IETS radiation resistance of the corresponding nucleotides. Previous radiation experiments on the purine and pyrimidine bases alone also show this same order of radiation damage and suggest that the quantum yields for UV radiation of pyrimidine compounds are a factor of ten greater than observed for purine compounds.

The UV damage to the isolated base residues was carried out only for cytosine and orotic acid which have resonance energies per π electron of 0.23β and 0.17β, respectively ($\beta \approx 16$ kcal/mole). Cytosine appears to be slightly more resistant to UV damage as measured by the persistence of the aromatic C–H stretching mode and several strong ring deformation modes as would be expected from the order of the resonance energies. Both of these bases have considerably lower resonance energies than adenine (see Table VI) and should be more

This article is copyrighted as indicated in the article. Reuse of AIP content is subject to the terms at: http://scitation.aip.org/termsconditions. Downloaded to IP: 128.83.63.20 On: Thu, 27 Nov 2014 09:56:33

TABLE VI.[a] Resonance energies of the biologically essential purines and pyrimidines (in units $\beta \approx 16$ kcal/mole).

Compound	Resonance energy	Number of π electrons[b]	Resonance energy per π electron	Ref.
Adenine	3.89	12	0.32	c, d
Guanine	3.84	14	0.27	c, d
Hypoxanthine	3.39	12	0.28	d
Xanthine	3.48	14	0.25	d
Uric acid	3.37	16	0.21	e
Cytosine	2.28	10	0.23	f
Uracil	1.92	10	0.19	f
Thymine	2.05	12	0.17	f
5-methylcytosine	2.41	12	0.20	f
Orotic acid	2.35	14	0.17	f
Barbituric acid	1.74	12	0.15	f

[a]Table from Ref. 20.
[b]Including hyperconjugation, when present.
[c]A. Pullman, B. Pullman, and G. Berthier, C. R. Acad. Sci. **243**, 380 (1956).
[d]A. Pullman and B. Pullman, Bull. Soc. Chim. France 766 (1958).
[e]A. Pullman and B. Pullman, C. R. Acad. Sci. **246**, 1613 (1958).
[f]A. Pullman and B. Pullman, Bull. Soc. Chim. France **594**, (1959).

easily damaged although as pointed out both are more resistant than the corresponding nucleotides formed with these base residues.

The correlation of the UV damage with resonance energy was further tested by irradiating *p*-chlorobenzoic acid adsorbed on the alumina substrate. The combination of higher resonant energy for benzene derivatives[21] and lower oscillator strengths for the $\pi\pi^*$ singlet transition should make them more resistant to radiation than aromatic heterocyclic derivatives such as the purines and pyrimidines. This is confirmed in the results of a 60 min UV exposure for *p*-chlorobenzoic acid as shown in Fig. 19. Very little modification of the vibrational spectrum is observed and no modes have undergone a selective intensity reduction as observed for the purines and pyrimidines.

Other electronic structural features (bond order, free valence, electrical charge, etc.) which relate to the reactivity of the bases toward free radical substitution also influence radiation resistance. These parameters have been calculated for the ground states of the purine and pyrimidine bases, but their exact significance to molecular damage by nonionizing radiation is uncertain since the excited state is the primary reaction state of the molecule. The absence of a reactive medium in the IETS experiments makes these later factors relatively unimportant so that a detailed separation of these factors is not needed.

As pointed out in the experimental section the rapid depletion of the skeletal ring vibration intensity indicates that the internal structure of the pyrimidine ring is damaged more rapidly than the double bond structure. This is in contrast to results on pyrimidines radiated[21] in aqueous solution or in air where the initiating step is nucleophilic attack at the carbon 5, 6 double bond resulting in saturation of the bond. This observation lends support to the conclusion that the radiation environment in the IETS experiments is relatively inert compared to those normally used in such radiation damage studies.

Hall *et al.*[5] have recently used IETS to study radiation damage in organic molecules by 30 keV electrons. Their results also show that the resonance energy per π electron correlates well with the relative resistance to damage of aromatic rings, conjugated rings and straight chain compounds. The resonance energy is highest for aromatic rings smaller for conjugated rings and smallest for straight chains. The cross sections for damage are found to increase rapidly for representative compounds in the above groups as the resonance energy decreases in the above order.

By measuring the peak height for selected modes as a function of exposure time as shown in Fig. 20 we have made rough quantitative estimates of the relative constituent damage rate in AMP and UMP. In UMP after

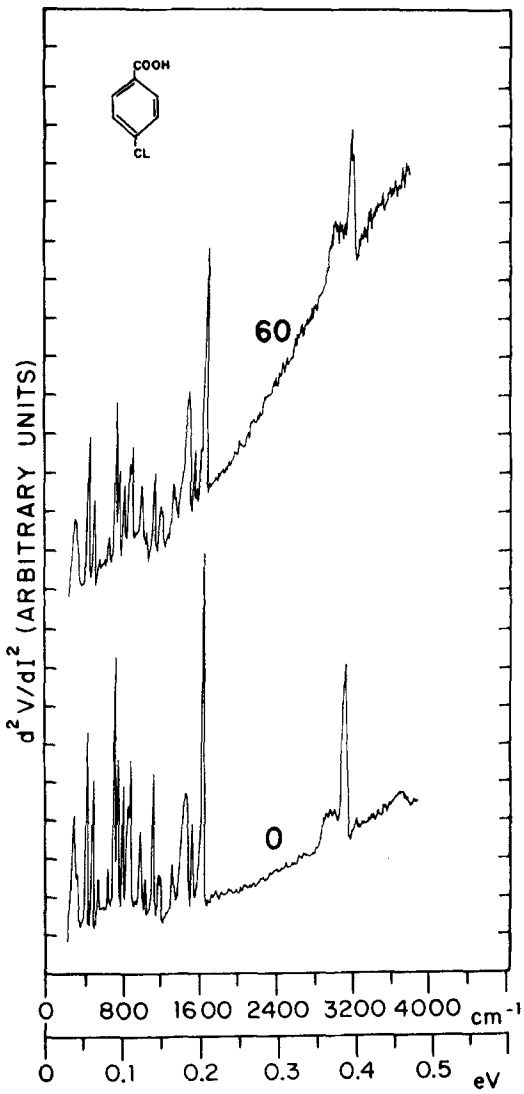

FIG. 19. UV radiation of *p*-chlorobenzoic acid. (0) Control spectrum, 277 Ω. (60) 60 min exposure, 200 Ω. Only a slight reduction of the mode intensity is observed as expected due to the higher resonance energy per π electron. Spectra were recorded at 4.2 K from junctions doped from an ethanol solution.

This article is copyrighted as indicated in the article. Reuse of AIP content is subject to the terms at: http://scitation.aip.org/termsconditions. Downloaded to IP: 128.83.63.20 On: Thu, 27 Nov 2014 09:56:33

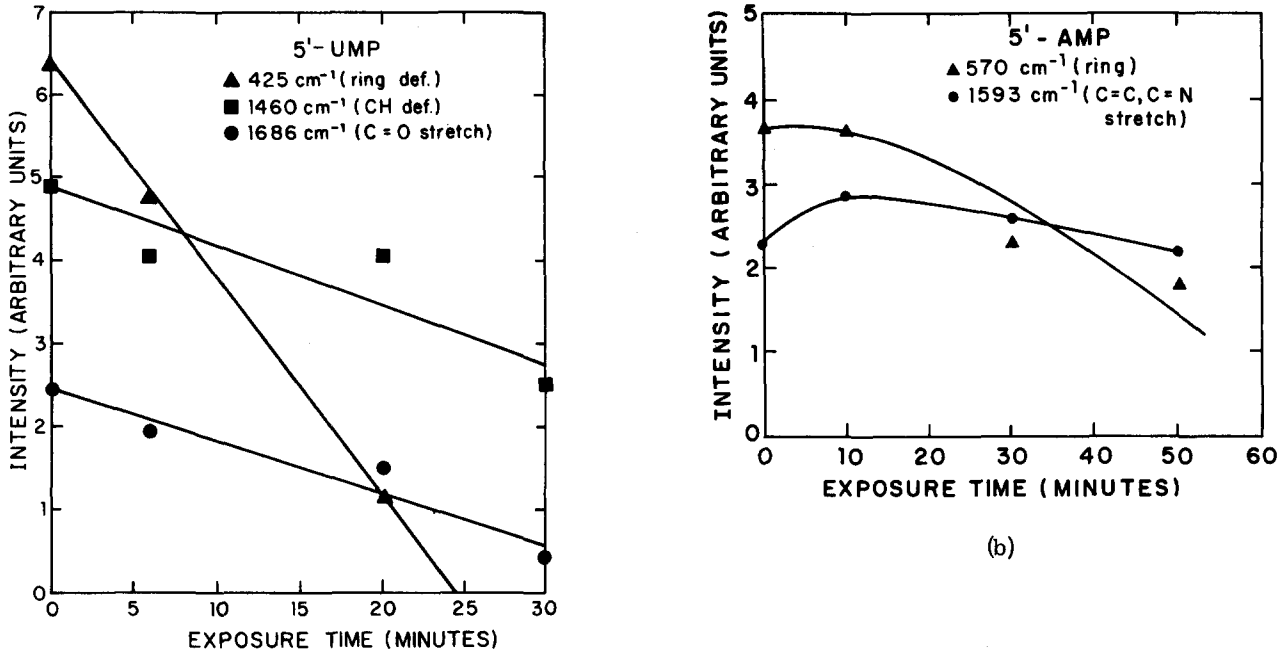

FIG. 20. Vibrational mode intensity as a function of UV exposure time. (a) Three selected modes for 5′-UMP. Damage rate is greatest for the ring deformation mode at 425 cm^{-1}. (b) Selected modes for 5′-AMP. Damage rates are lower than in 5′-UMP and double bond stretch mode at 1593 cm^{-1} shows practically no reduction in intensity over a 50 min exposure time.

a 20 min exposure to UV the ring deformation mode at 428 cm^{-1} showed an 80% reduction in intensity, the C=O stretch mode at 1686 cm^{-1} a 50% reduction and the CH deformation mode at 1460 cm^{-1} a 28% reduction. These values alone clearly indicate that the base ring bond structure damages first while the CH components of the molecule are most resistant to radiation damage.

AMP is substantially more resistant to radiation and in this case after a 40 min exposure to UV the ring deformation mode at 570 cm^{-1} is reduced in intensity by 40% while the double bond modes show little if any change in intensity [see Fig. 20(b)]. This later observation is partially due to the growth of additional double bond structure during irradiation of AMP which definitely, distinguishes the purine base nucleotides from the pyrimidine base nucleotides. UV radiation of the more complex purine rings may give fragments with more double bond structure and a stronger decoupling of existing double bond modes may also occur.

The CH mode structure generally remains quite strong throughout the radiation sequence for both purine and pyrimidine nucleotides and contributes the dominant modes in the spectrum following maximum irradiation. This result is reasonable and results from a combination of two factors. The CH groups themselves are the least damaged by UV and the ring breaks probably produce fragments with aliphatic CH components. Tracking the aromatic CH versus the aliphatic CH intensity by observing the CH stretching region is difficult since the nucleotides contain both components and initial aliphatic C–H stretching modes contribute greater intrinsic IETS intensity.

C. UV damage mechanisms in nucleotides

The most notable reaction of biological importance is photodimerization[22] of the nucleotides during irradiation. Dimer formation occurs when two of the bases become linked together by a cyclobutane ring formed across the carbon 5, 6 double bonds. Dimer formation depends strongly on the appropriate steric orientation of the two bases and is most easily observed in frozen aqueous solutions where the bases aggregate. We do not detect dimer formation in the IETS experiments which is again consistent with the IETS method which fixes the isolated mononucleotide on the alumina surface. Adsorption of polynucleotides may increase the possibility of reaction between adjacent nucleotides although an initial UV irradiation on poly UMP shows the same damage sequence as observed for the mononucleotide as shown in Fig. 21. The photoreaction favoring dimer formation is optimal in the wavelength range $\lambda = 2600$–2800 Å and can be reversed with radiation below 2400 Å. Marcus and Corelli[23] irradiated bulk films of uracil and thymine at $\lambda = 2537$ Å and from the infrared spectra identified the formation of dimers from the development of a mode at 1280 cm^{-1}. By using a monochromator ahead of our light source we irradiated UMP molecules on the alumina substrate at $\lambda = 2537$ and for exposures up to several hours and no evidence of dimer formation was detected providing further evidence that the steric conditions for the molecules adsorbed on alumina are not favorable for dimer formation. It is probable that nucleotide layers thicker than a monolayer will be necessary in order to examine possible dimer formation with IETS.

The radiation fluence incident on the adsorbed layer for a one minute exposure time is 1.26×10^{19} photons/

This article is copyrighted as indicated in the article. Reuse of AIP content is subject to the terms at: http://scitation.aip.org/termsconditions. Downloaded to IP: 128.83.63.20 On: Thu, 27 Nov 2014 09:56:33

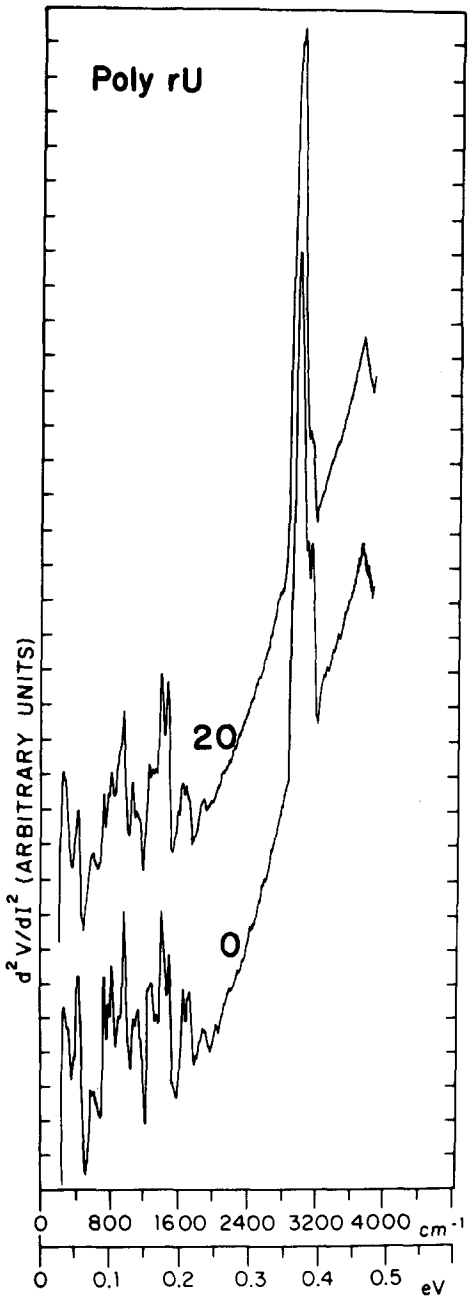

FIG. 21. UV radiation of polyuridylic acid. (0) Control spectrum, 689 Ω. (20) 20 min exposure, 500 Ω. Damage is similar to that observed for the mononucleotide 5′-UMP. No dimer formation is observed.

cm^2 assuming an average wavelength of 2500 Å. The saturated monolayer coverage of the barrier is estimated[24,25] to be 5×10^{14} molecules/cm^2. Therefore ~2.5 $\times10^4$ photons/min are incident on each molecule.

At present we have no estimate of the molar adsorptivity of the molecules when adsorbed on the aluminum oxide barrier. The surface molecular interaction and the presence of the aluminum metal electrode at a distance small compared to the optical wavelength may change the molar adsorptivity substantially from that measured for molecules in bulk or in solution.

If the published[26] values of molar absorptivity are used then a cross section for the excitation of a $\pi\pi^*$ state can be calculated and used to obtain an estimate of ~60 photons/min adsorbed per molecule. The excited singlet states of the nucleotides have lifetimes[27] of the order of 10^{-7} sec while the triplet states have lifetimes in the range 10^{-2} to 10 sec (with a lower occupation probability). Therefore, in the absence of dissociative reactions involving the excited state the primary damage event is a direct photon-induced bond break from the ground state of the molecule.

If the quantum yield for such an event is on the order of 0.001 (the cross-section ratio $\sigma_{ex}/\sigma_{bb}\approx1000$) then assuming 60 photons/min adsorbed exposure times of several minutes or more would be required to detect damage. This seems to be in agreement with the experimental observations, but should be considered as speculative due to the uncertainty in the molar absorptivity.

We have also compared radiation damage to cytosine and CMP using IETS and as pointed out in reference to Fig. 14 the nucleotide damages more rapidly than the isolated base. The *D*-ribose is an electron withdrawing substituent when attached to the base ring and this electronic modification is probably responsible for the greater radiation sensitivity of the nucleotide. Examination of the IETS in the radiation sequence for CMP indicates that the *D*-ribose has not been cleaved from the base by UV exposure. The spectrum remains characteristic of the combined sugar and base rather than shifting toward either the *D*-ribose or base residue spectrum. Comparison for the other base residues and nucleotides with IETS is more difficult since the isolated base residues are very weakly chemisorbed on alumina and final concentrations sufficient for the UV studies are difficult to obtain.

D. UV radiation effects on surface structure

All IETS spectra show a broad peak at 900–1000 cm^{-1} which is attributed to the excitation of phonons in the alumina barrier. For an undoped junction this peak has a very characteristic shape as shown in Fig. 22. The junction in this case has been overoxidized to give a relatively high resistance barrier so that a full spectrum can be obtained. The CH mode frequencies are contributed from a small amount of hydrocarbon contamination and are eliminated for junctions prepared under the ultra high vacuum conditions used in the present experiments.

For the junctions doped with nucleotides the phonon modes of the alumina barrier contribute a background intensity in the frequency range 800–1000 cm^{-1} while fairly intense modes from the base rings are superimposed on this background. As the UV radiation dose is increased the base ring modes show a substantial reduction in intensity while the aluminum phonon modes become relativity enhanced. Structure on the lower side of the aluminum phonon maximum develops during irradiation so that the final broad peak is identical to that observed for the undoped junctions. This development can be followed in the radiation sequence for CMP or dTMP as shown in Figs. 9 and 8.

Although these changes are not directly coupled to the

This article is copyrighted as indicated in the article. Reuse of AIP content is subject to the terms at: http://scitation.aip.org/termsconditions. Downloaded to IP: 128.83.63.20 On: Thu, 27 Nov 2014 09:56:33

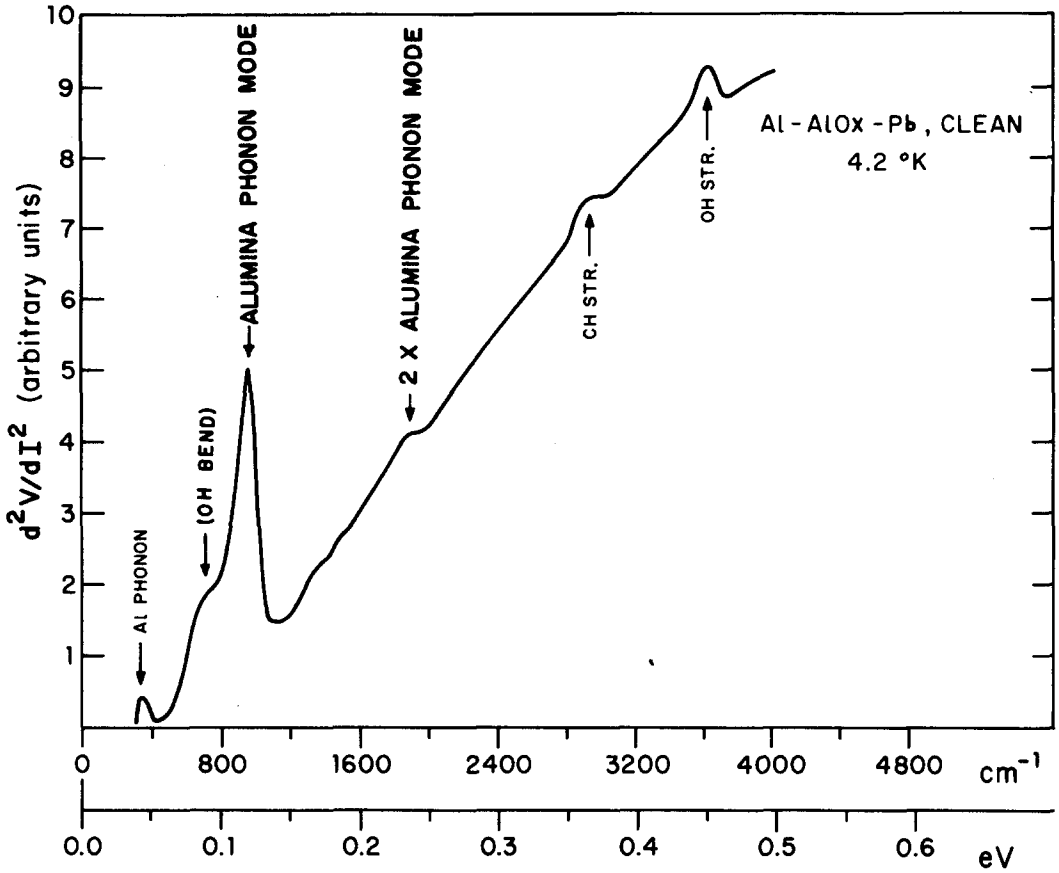

FIG. 22. IETS spectrum of undoped Al–AlO_x–Pb junction. The broad peak centered just above 900 cm^{-1} is associated with the aluminum oxide phonon modes. This is a relatively strong feature in the late stages of UV damage due to quenching of the ring modes in the same region.

nucleotide damage they do indicate that the surface reaction sites are changed to some degree as the base ring of the nucleotide is fragmented. This is consistent with the weak chemisorption of the base ring and also suggests that the broad aluminum phonon modes can be assigned to modes that involve the surface reaction sites of the alumina and that both the intensity and line shape are influenced by the specific molecular interaction.

If a strong bonding group such as COOH is substituted on the base ring then the relative development of the alumina phonon modes during irradiation is not observed as pointed out for ortic acid in Fig. 15. In this case the strongly adsorbed CO_2 carboxylate ion structure and coupled surface alumina phonon structure is apparently unchanged by the UV irradiation even though the ortic acid ring modes are substantially damaged during a 50 min UV irradiation.

As discussed in reference to *D*-ribose in Fig. 16 the cooled substrate enhances and downshifts the OH stretching vibration associated with the surface active sites. After a 40 min UV exposure the OH stretching mode is restored to the higher frequency position and reduced in intensity. These shifts are on the order of 130 cm^{-1} and represent a substantial modification of the surface active site structure. This is only indirectly related to the molecular UV damage but demonstrates the high sensitivity of the IETS technique to detailed surface modification.

VI. CONCLUSIONS

The results reported in this paper show that the inelastic electron tunneling technique provides a systematic method for studying the primary bond damage in nucleotides and other biological molecules due to UV irradiation. The special conditions resulting from the adsorption of one monolayer of molecules on the aluminum oxide substrate and the subsequent irradiation in a vacuum environment prevent any appreciable secondary reaction. The surface reaction influences selected groups such as the PO_2^- group on the nucleotides but generally leaves the vibrational spectrum of the molecule unchanged from that of the molecule in the solid state or solution. The surface configuration of the nucleotides provides a very stable temperature independent IETS spectrum which we interpret as resulting from the constraints on the surface adsorption due to the orientation of the base and sugar rings. Other compounds such as peptides show a greater spectral sensitivity to temperature and surface orientation and these effects although completely reproducible must be taken into account in calibrating the UV damage as determined from IETS spectra.

In the case of the nucleotides the UV damage rate is determined by the base residue and the order of damage is the same as that reported for the isolated bases. In the IETS studies the relative order of observed damage rate for the nucleotides studied is

This article is copyrighted as indicated in the article. Reuse of AIP content is subject to the terms at: http://scitation.aip.org/termsconditions. Downloaded to IP: 128.83.63.20 On: Thu, 27 Nov 2014 09:56:33

UMP > dTMP > CMP > GMP > AMP .

This order correlates in inverse order with the calculated resonance energies per π electron for the base residues involved which are listed as 0.19β, 0.17β, 0.23β, 0.27β, and 0.32β for *U*, *T*, *C*, *G*, and *A*, respectively, where $\beta \approx 16$ kcal/mole. The direct bond breaking rate should be highest for the lowest resonance energy since delocalization is less and decay of the excitation energy through nondissociative channels is less likely.

UV damage to only two bases cytosine and 6-carboxyuracil has so far been studied using IETS. In these cases the base is more resistant to UV damage than is the corresponding nucleotide. This suggests that the addition of the sugar and phosphate groups lowers the resonance energy of the base although the base is still the major factor in determining the UV damage rate in the nucleotides. The base pairing through hydrogen bonding in nucleic acid forms large conjugated units with molecular orbitals extending over the whole of the surface covered by the base pairs and adds substantial resonance energy which will be expected to stabilize the molecule against UV damage. So far we have not used IETS to study UV damage in larger nucleic acid units but the IETS technique is definitely applicable to these molecules.[9]

We have not observed the formation of dimers in the present experiments and this is consistent with the low density isolated molecular layer fabricated for the IETS experiments. Dimer formation is more characteristic in bulk films or frozen aqueous solutions with aggregated bases. More concentrated thin film barriers can be fabricated for the IETS experiments, but this will require further development work.

The present experiments have shown that the IETS technique is generally applicable to the detection of UV damage to surface adsorbed molecules. No problems have resulted from exposing the surface adsorbed monolayer to ultra high vacuum for many hours before deposition of the lead counter electrode. It has been discovered that for certain molecules the intensity of the IETS spectrum is quite sensitive to the substrate temperature at which the lead electrode is evaporated. After evaporation of the counterelectrode no further spectral changes can be introduced. Further applications to surface chemistry and photochemistry look promising and the technique provides high sensitivity for monolayer studies.

ACKNOWLEDGMENTS

This research was supported in part by the National Science Foundation and the Department of Energy. An equipment grant from the University of Virginia Research Policy Council is gratefully acknowledged. The authors have received important help from Estelle Phillips in technical aspects of the junction preparation and measurement. Useful discussions have been held with Professor J. E. Coleman, Professor P. K. Hansma, and Dr. C. S. Korman.

[1] R. B. Setlow and W. L. Carrier, J. Mol. Biol. **17**, 237 (1966).
[2] R. B. Setlow, Science **153**, 379 (1966).
[3] M. Parikh, J. T. Hall, and P. K. Hansma, Phys. Rev. A **14**, 1437 (1976).
[4] M. G. Simonsen, Ph.D. thesis (University of Virginia, 1974) (unpublished).
[5] J. T. Hall, P. K. Hansma, and M. Parikh, Surf. Sci. **65**, 552 (1977).
[6] J. R. Kirtley and P. K. Hansma, Phys. Rev. B **12**, 531 (1975).
[7] M. G. Simonsen, R. V. Coleman, and P. K. Hansma, J. Chem. Phys. **61**, 3789 (1974).
[8] P. K. Hansma, Phys. Rep. **30**, 146 (1977).
[9] R. V. Coleman, J. M. Clark, and C. S. Korman, in *Inelastic Electron Tunneling Spectroscopy*, edited by T. Wolfram (Springer, New York, 1978), p. 34.
[10] P. K. Hansma and R. V. Coleman, Science **184**, 1369 (1974).
[11] R. C. Lord and G. J. Thomas, Jr., Spectrochim. Acta Part A **23**, 2551 (1967).
[12] H. Susi and J. S. Ard, Spectrochim. Acta Part A **27**, 1549 (1971).
[13] J. M. Clark and R. V. Coleman, Proc. Natl. Acad. Sci. USA **73**, 1598 (1976).
[14] H. Susi, J. S. Ard and J. M. Purcell, Spectrochim. Acta Part A **29**, 725 (1973).
[15] C. L. Angell, J. Chem. Soc. 504 (1961).
[16] A. D. McLaren and D. Shugar, *Photochemistry of Proteins and Nucleic Acids* (Pergamon, New York, 1964).
[17] M. Guéron, J. Eisinger, and A. A. Lamola, in *Basic Principles in Nucleic Acid Chemistry*, edited by P. O. P. Ts'o (Academic, New York, 1974), Vol. I, p. 312.
[18] C. S. Korman, J. C. Lau, A. M. Johnson, and R. V. Coleman, Phys. Rev. B **19**, 994 (1979).
[19] P. O. P. Ts'o, in *Basic Principles in Nucleic Acid Chemistry*, edited by P. O. P. Ts'o (Academic, New York, 1974), Vol. I, p. 481.
[20] A. Pullman and B. Pullman, in *Comparative Effects of Radiation*, edited by M. Burton, J. S. Kirby-Smith, and J. L. Magee (Wiley, New York, 1960), p. 105; B. Pullman and A. Pullman, *Quantum Biochemistry* (Interscience, New York, 1963), p. 184.
[21] K. C. Smith and P. C. Hanawalt, *Molecular Photobiology* (Academic, New York, 1969).
[22] R. Beukers and W. Berends, Biochim. Biophys. Acta **41**, 550 (1960).
[23] M. A. Marcus and J. Corelli, Radiat. Res. **57**, 20 (1974).
[24] J. B. Peri, J. Phys. Chem. **69**, 220 (1965).
[25] J. D. Langan and P. K. Hansma, Surf. Sci. **52**, 211 (1975).
[26] M. Guéron, J. Eisinger, and R. G. Schulman, J. Chem. Phys. **47**, 4077 (1967).
[27] W. M. Horspool, *Aspects of Organic Photochemistry* (Academic, New York, 1976).

This article is copyrighted as indicated in the article. Reuse of AIP content is subject to the terms at: http://scitation.aip.org/termsconditions. Downloaded to IP: 128.83.63.20 On: Thu, 27 Nov 2014 09:56:33